Gene regulatory network architecture in different developmental contexts influences the genetic basis of morphological evolution

Sebastian Kittelmann[1], Alexandra D. Buffry[1], Isabel Almudi[2], Marianne Yoth[1], Gonzalo Sabaris[3], Franziska A. Franke[1], Juan Pablo Couso[2], Maria D. S. Nunes[1], Nicolás Frankel[3], José Luis Gómez-Skarmeta[2], Jose Pueyo-Marques[4], Saad Arif[1,#] and Alistair P. McGregor[1,#]

[1] Department of Biological and Medical Sciences, Oxford Brookes University, Gipsy Lane, Oxford UK OX3 0BP.
[2] Centro Andaluz de Biología del Desarrollo, CSIC/ Universidad Pablo de Olavide, Carretera de Utrera Km1, 41013 Sevilla, Spain.
[3] Departmento de Ecologia, Genetica y Evolucion, IEGEBA-CONICET, Facultad de Ciencias Exactas y Naturales, Universidad de Buenos Aires, Buenos Aires, Argentina.
[4] Brighton and Sussex Medical School, University of Sussex, East Sussex, Falmer, Brighton BN1 9PS, UK.

Corresponding authors

Keywords: development, evolution, gene regulatory networks, *Drosophila*, gene expression.

Abstract

Convergent phenotypic evolution is often caused by recurrent changes at particular nodes in the underlying gene regulatory networks (GRNs). The genes at such evolutionary 'hotspots' are thought to maximally affect the phenotype with minimal pleiotropic consequences. This has led to the suggestion that if a GRN is understood in sufficient detail, the path of evolution may be predictable. The repeated loss of larval trichomes among *Drosophila* species is caused by the loss of *shavenbaby* (*svb*) expression. *svb* is also required for development of leg trichomes, but the evolutionary gain of trichomes in the 'naked valley' on T2 femurs in *Drosophila melanogaster* is caused by the loss of *microRNA-92a* (*miR-92a*) expression rather than changes in *svb*. We compared the architectures of the larval and leg trichome GRNs to investigate why the genetic basis of trichome pattern evolution differs in these developmental contexts. We found key differences between these two networks in both the genes employed, and in the regulation and function of common genes. These differences in the GRNs reveal why mutations in *svb* are unlikely to contribute to leg trichome evolution and how instead *miR-92a* represents the key evolutionary switch in this context. Our work shows that differences in the components and wiring of GRNs in different developmental contexts, as well as whether a morphological feature is lost versus gained, influence the nodes at which a GRN evolves to cause morphological change. Therefore our findings have important implications for understanding the pathways and predictability of evolution.

Significance Statement

A major goal of biology is to identify the genetic cause of organismal diversity. Convergent evolution of traits is often caused by changes in the same genes – evolutionary 'hotspots'. *shavenbaby* is a 'hotspot' for larval trichome loss in *Drosophila*, however *microRNA-92a* underlies the gain of leg trichomes. To understand this difference in the genetics of phenotypic evolution, we compared the underlying gene regulatory networks (GRNs). We found that differences in GRN architecture in different developmental contexts, and whether a trait is lost or gained, influence the pathway of evolution. Therefore hotspots in one context may not readily evolve in a different context. This has important implications for understanding the genetic basis of phenotypic change and the predictability of evolution.

Introduction

A major challenge in biology is to understand the relationship between genotype and phenotype, and how genetic changes modify development to generate phenotypic diversification. The genetic basis of many phenotypic differences within and among species have been identified (e.g. 1, 2-15), and these findings support the generally accepted hypothesis that morphological evolution is predominantly caused by mutations affecting *cis*-regulatory modules of developmental genes (16). Moreover, it has been found that changes in the same genes commonly underlie the convergent evolution of traits (reviewed in 17). This suggests that there are evolutionary 'hotspots' in GRNs: changes at particular nodes are repeatedly used during evolution because of the role and position of the gene in the GRN, and the limited pleiotropic effect of the change (18-21).

The regulation of trichome patterning is an excellent system for studying the genetic basis of evolutionary morphological change (22). Trichomes are actin protrusions from epidermal cells that are overlaid by cuticle and form short, non-sensory, hair-like structures. They can be found on various parts of insect bodies during different life stages, and are thought to be involved in, for example, thermo-regulation, aerodynamics, oxygen retention in semi-aquatic insects, grooming, and larval locomotion (23-27) (Fig. 1).

The GRN underlying trichome formation on the larval cuticle of *Drosophila* species has been characterised in great detail (reviewed in 21, 22, 28) (Fig. 1). Several upstream transcription factors, signalling pathways, and *tarsal-less* (*tal*)-mediated post-translational proteolytic processing lead to the activation of the key regulatory transcription factor Svb, which, with SoxNeuro (SoxN), activates a battery of downstream effector genes (6, 29-35). These downstream factors modulate cell shape changes, actin polymerisation, or cuticle segregation, which underlie the actual formation of trichomes (30, 35). Importantly, ectopic activation of *svb* during embryogenesis is sufficient to drive trichome development on otherwise naked larval cuticle, and loss of *svb* function leads to a loss of larval trichomes (36).

Regions of dorso-lateral larval trichomes have been independently lost at least four times among *Drosophila* species (37, 38). In all cases, this phenotypic change is caused by changes in *svb* enhancers, resulting in a loss of *svb* expression (13-15, 37-39). The modular enhancers of *svb* are thought to allow the accumulation of mutations that facilitate the loss of certain larval trichomes without deleterious pleiotropic consequences. Note, however, that evolved enhancers underlying differences in larval trichomes also drive expression in other tissues (40). It is thought that changes in larval trichome patterns cannot be achieved by mutations in genes upstream of *svb* because of deleterious pleiotropic effects, while changes in individual *svb* target genes would only affect trichome morphology rather than their presence or absence (19-21, 30, 35). Given the position and function of *svb* in the larval trichome GRN, these data suggest that *svb* is a hotspot for the evolution of trichome patterns more generally because it is also required for the formation of trichomes in adult epidermis and can induce ectopic trichomes on wings when over expressed (36, 40). Therefore, one could predict that changes in adult trichome patterns are similarly achieved through changes in *svb* enhancers (20, 21).

The trichome pattern on femurs of second legs varies within and between *Drosophila* species (1, 41) (Fig. 1). In *D. melanogaster*, an area of trichome-free cuticle or 'naked valley' varies in size among strains from small to larger naked valleys. Other species of the *D. melanogaster* species subgroup only exhibit larger naked valleys (1, 41). Therefore trichomes have been gained at the expense of naked cuticle in some strains of *D. melanogaster*. Differences in naked valley size between species have been associated with differences in the expression of *Ultrabithorax* (*Ubx*), which represses the formation of leg trichomes (41). However, smaller naked valley size in populations of *D. melanogaster* is caused by a reduction of *miR-92a* expression, which represses trichome formation by repressing the *svb* target gene *shavenoid* (*sha*) (1, 42). Therefore, while *svb* is thought to be a hotspot for the evolutionary loss of patches of larval trichomes, it does not appear to underlie the evolutionary the gain of leg trichomes in *D. melanogaster*.

Differences in GRN architecture among developmental contexts may affect which nodes can evolve to facilitate phenotypic change in different tissues or developmental stages. In addition, an evolutionary gain or loss of a phenotype may also result from changes at different nodes in the underlying GRN, i.e. alteration of a particular gene may allow the loss of a trait but changes in the same gene may not necessarily result in the

gain of the same trait. Therefore, a better understanding of the genetic basis of phenotypic change and evaluation of the predictability of evolution requires characterising GRN architecture in different developmental contexts and studying how the loss versus the gain of a trait is achieved.

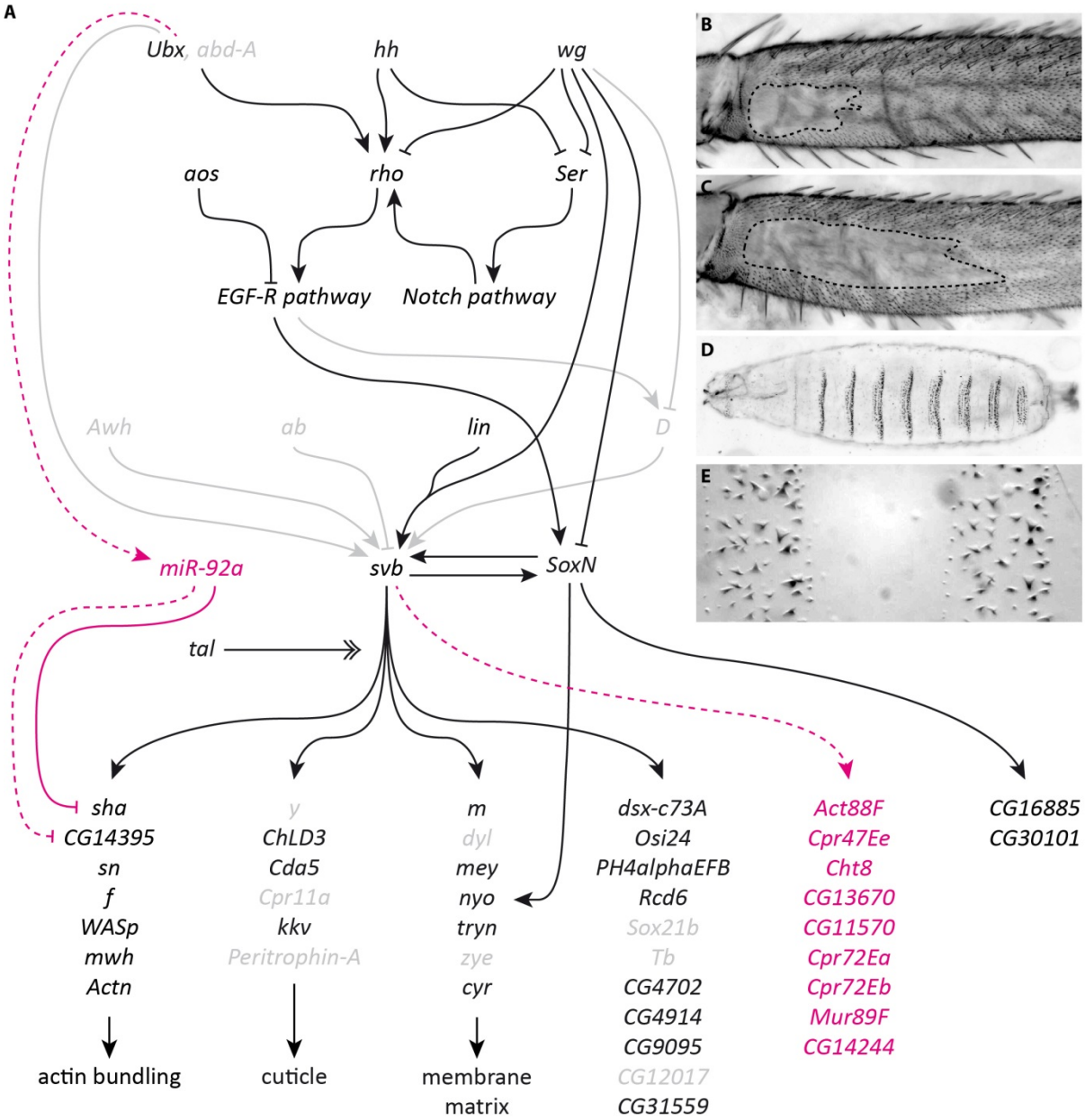

Figure 1: The GRN controlling formation of trichomes on larval and leg epidermis differs between these developmental contexts. (A) The GRN is well understood for larval trichome development (22, 30, 75, 76). Grey shading indicates that a gene is not expressed above threshold in legs (and therefore its interactions are not present). Magenta colour indicates presence only during leg development. Dotted lines indicate likely interactions. Expression of *svb* is controlled by several upstream transcription factors and signalling pathways, but some of them are not active during leg trichome development. Activation of Svb protein requires proteolytic cleavage by small peptides encoded by *tal* (6, 31, 77). Active Svb then regulates the expression of over 150 target genes (30, 35) of which a subset is shown. The products of these downstream genes are involved in actin bundling, cuticle segregation, or changes to the matrix, which lead to the actual formation of trichomes. SoxN and Svb activate each other and act partially redundantly on downstream targets (33, 34). *miR-92a* is only expressed in naked valley cells where it represses *sha* and possibly *CG14395* and thereby acts as a short circuit for *svb*. Its expression is likely controlled by *Ubx*. (B, C) A trichome-free region on the posterior of the T2 femur differs in size between different strains. Shown are *OregonR* (B) and e^4,wo^1,ro^1 (C). (D, E) Trichomes on the ventral side of the larval cuticle form stereotypic bands ('denticle belts') separated by trichome-free cuticle.

Here we report our comparison of the GRN underlying trichome development in legs versus embryos. Our results show that differences in GRN composition and architecture in these two developmental contexts

mean that it is likely *svb* is unable to act as a switch for the gain of leg trichomes because it is already expressed throughout the legs in both naked and trichome-producing cells. Instead, regulation of *sha* by *miR-92a* appears to act as the switch between naked and trichome-producing cells in the leg. This shows that the architecture of a GRN in different developmental contexts can affect the pathway used by evolution to generate phenotypic change.

Materials and Methods

Fly strains, husbandry and crosses

Fly strains used in this study are listed in Table S1. Flies were reared on standard food at 25 °C if not otherwise indicated.

Replacement of the P{lacW}l(3)S011041 element, which is inserted 5' of the *tal* gene, by a P{GaWB} transposable element was done by mobilization in *omb-Gal4; +/CyO Δ2–3; l(3)S011041/TM3Sb* flies as described in Galindo, Pueyo, Fouix, Bishop and Couso (32). Replacements were screened by following *UAS-GFP* expression in the progeny. The P{GaWB} element is inserted in the same nucleotide position as P{lacW}S011041. Clonal analysis of *tal* S18.1 and *svbR9* alleles were performed as described in Pueyo and Couso (43).

A transgenic line that contains the *cis*-regulatory region of *svb* upstream of a GFP reporter (*svb*BAC-GFP) (40) was used to monitor *svb* expression. Legs of pupae were dissected 24 h after puparium formation (hAPF), fixed and stained following the protocol of Halachmi et al. (2012) (44), using a chicken anti-GFP as primary antibody (Aves Labs, 1:250) and an anti-chicken as secondary (AlexaFluor 488, 1:400). Images were obtained on a confocal microscope with a 60X objective. SUM projections of the z-stacks were generated after background subtraction. A filter median implemented in ImageJ software (http://rsb.info.nih.gov/ij/) was applied. The proximal femur image was reconstructed from two SUM projections using Adobe Photoshop.

RNA-seq

Pupae were collected within 1 hAPF and allowed to develop for another 20 to 28 h at 25 °C. Second legs were dissected in PBS from approximately 80 pupae per replicate and kept in RNAlater. RNA was isolated using phenol-chloroform extraction. This was done in three replicates for two different strains (e^4,wo^1,ro^1 and OregonR). Library preparation and sequencing (75 bp paired end) were carried out by Edinburgh Genomics. Reads were aligned to *D. melanogaster* genome version 6.12 (45) using TopHat (46). Transcriptomes were assembled using Cufflinks and analysed using Cuffdiff (47) (Supplementary Files 1-7). Genes expressed below 1 FPKM were considered not expressed. The raw reads will be deposited in the Gene Expression Omnibus.

ATAC-seq

Pupae were reared and dissected as described above. Dissected legs were kept in ice cold PBS. Leg cells were lysed in 50 µl Lysis Buffer (10 mM Tris-HCl, pH = 7.5; 10 mM NaCl; 3 mM $MgCl_2$; 0.1 % IGEPAL). Nuclei were collected by centrifugation at 500 g for 5 min. Approximately 60,000 nuclei were resuspended in 50 µl Tagmentation Mix [25 µl Buffer (20 mM Tris-CH_3COO^-, pH = 7.6; 10 mM $MgCl_2$; 20 % Dimethylformamide); 2.5 µl Tn5 Transposase; 22.5 µl H_2O] and incubated at 37 °C for 30 min. After addition of 3 µl 2 M NaAC, pH = 5.2 DNA was purified using a QIAGEN MinElute Kit. PCR amplification for library preparation was done for 15 cycles with NEBNext High Fidelity Kit; primers were used according to (48). This procedure was repeated for three replicates in each of two strains (e^4,wo^1,ro^1 and OregonR). Paired end 50 bp sequencing was carried out by the Transcriptome and Genome Analysis Laboratory Göttingen, Germany. Reads were end-to-end aligned to *D. melanogaster* genome version 6.12 (FlyBase) (45) using bowtie2 (49). After filtering of low quality reads and removal of duplicates using SAMtools (50, 51), reads were re-centered according to Buenrostro, Giresi, Zaba, Chang and Greenleaf (48). Peaks were called with MACS2 (52) and visualisation was done using Sushi (53) (Supplementary Files 8, 9).

Results

The composition of the leg trichome GRN differs from the larval trichome GRN

To better characterise the GRN underlying leg trichome development we first carried out RNA-Seq of T2 pupal legs between 20 and 28 hAPF, which is the window when leg trichomes are specified (41) (Supplementary File 1-6). We found that key genes known to be involved in larval trichome formation are expressed in legs. These include *Ubx, SoxN, tal, svb*, and *sha*, as well as key components of the Delta-Notch, Wnt and EGF signalling pathways (Table S2). However, we did not detect expression of *Dichaete, arrowhead* or *abrupt*, which are also known to regulate *svb* expression during larval trichome development (33, 39) (Table S2). Furthermore, we did not detect expression of 24 of the 163 known targets of *svb* in embryos (30, 35) in our dataset (Table S2). In addition, 10 out of the 43 genes thought to be involved in larval trichome formation independently of *svb* (34, 35) are not expressed in legs (Table S2). These changes in both Svb targets and other trichome effector genes possibly reflect differences in trichome morphology between larvae and legs (see 54). It also suggests that other factors, in addition to Svb, are required to activate these genes specifically during larval trichome development that are not used during leg trichome development. Alternatively, the Svb-dependent *cis*-regulatory elements of some of these genes may not be accessible during leg trichome formation. Overall, our RNA-Seq data exemplify differences in both upstream and downstream components of the leg trichome GRN when comparing it to the embryonic GRN that specifies larval trichomes.

We next compared our leg RNA-Seq data to published RNA-Seq datasets for embryos 12-14 and 14-16 h after egg lay (55). Svb activation during these developmental windows is critical for larval trichome formation (31). We identified a set of 105 genes expressed in our leg RNA-Seq data that showed little to no expression in embryos 12-16 hours AEL (Table S3). 94 of these 'leg-specific' genes are protein-coding while the other eleven produce non-coding RNAs. Gene ontology (GO) analysis of the protein-coding genes showed that nine are associated with chitin and cuticle development and hence may play a role in trichome formation, and a further five genes encode potential transcription factors (Table S3). Therefore, these genes represent candidates for the development of leg trichomes that are not used during larval trichome production.

Regulation of svb during leg trichome patterning

Given the important role of *svb* in trichome development and patterning, we investigated the regulatory sequences for this gene used in T2 legs. To do this we carried out ATAC-Seq (48, 56) on chromatin from T2 legs during the window of 20 to 28 hAPF when leg trichomes are specified.

Embryonic expression of *svb* underlying larval trichomes is regulated by several enhancers spanning a region of approximately 90 kb upstream of the transcription start site of this gene (15, 57) (Fig. 2). Several of these larval enhancers also drive reporter gene expression during pupal development (40). We observed that the embryonic enhancers DG3, E and 7 contained regions of open chromatin according to our T2 leg ATAC-Seq data. However, we found additional accessible chromatin regions that do not overlap with known embryonic *svb* enhancers (Fig. 2).

Deletion of a region including the embryonic enhancers DG2 and DG3 [Df(X)svb^{108}] (Fig. 2) results in a reduction in the number of dorso-lateral larval trichomes when in a sensitized genetic background or at extreme temperatures (57). Moreover, Preger-Ben Noon and colleagues (2017) (40) recently showed that this deletion, as well as a larger deletion that also removes embryonic enhancer A ([Df(X)svb^{106}], see Fig. 2), results in the loss of trichomes on abdominal segment A5, specifically in males. We found several peaks of open chromatin in the regions covered by these two deficiencies in our second leg ATAC-seq dataset (Fig. 2) and therefore tested the effect of Df(X)svb^{106} on leg trichome development. We found that deletion of this region and consequently enhancers DG2, DG3, Z and A did not affect the size of the naked valley or the density of trichomes on the femur or other leg segments of flies raised at 17°C, 25°C, or 29°C (compared to the parental lines) (Fig. S1). This suggests that while this region may contribute to *svb* expression in legs, its removal does not perturb the robustness of leg trichome patterning.

Next, to try to identify enhancer(s) responsible for leg expression, we employed all available GAL4 reporter lines for cis-regulatory regions of *svb* (Table S1) that overlap with regions of open chromatin

downstream of the above deficiencies (Fig. 2). All 10 regions that overlap with open chromatin are able to drive GFP expression to some extent in second legs between 20 and 28 hAPF, as well as in other pupal tissues (Fig. S2). While some of the regions only produce expression in a handful of epidermal cells or particular regions of the T2 legs, none are specific to the presumptive naked valley, and VT057066, VT057077, VT057081, and VT057083 appear to drive variable levels of GFP expression throughout the leg (Fig. S2). Note that the two regions overlapping with larval enhancers E and 7 (VT057062 and VT057075, respectively) only drive weak expression in a few cells in the tibia and tarsus (Fig. S2).

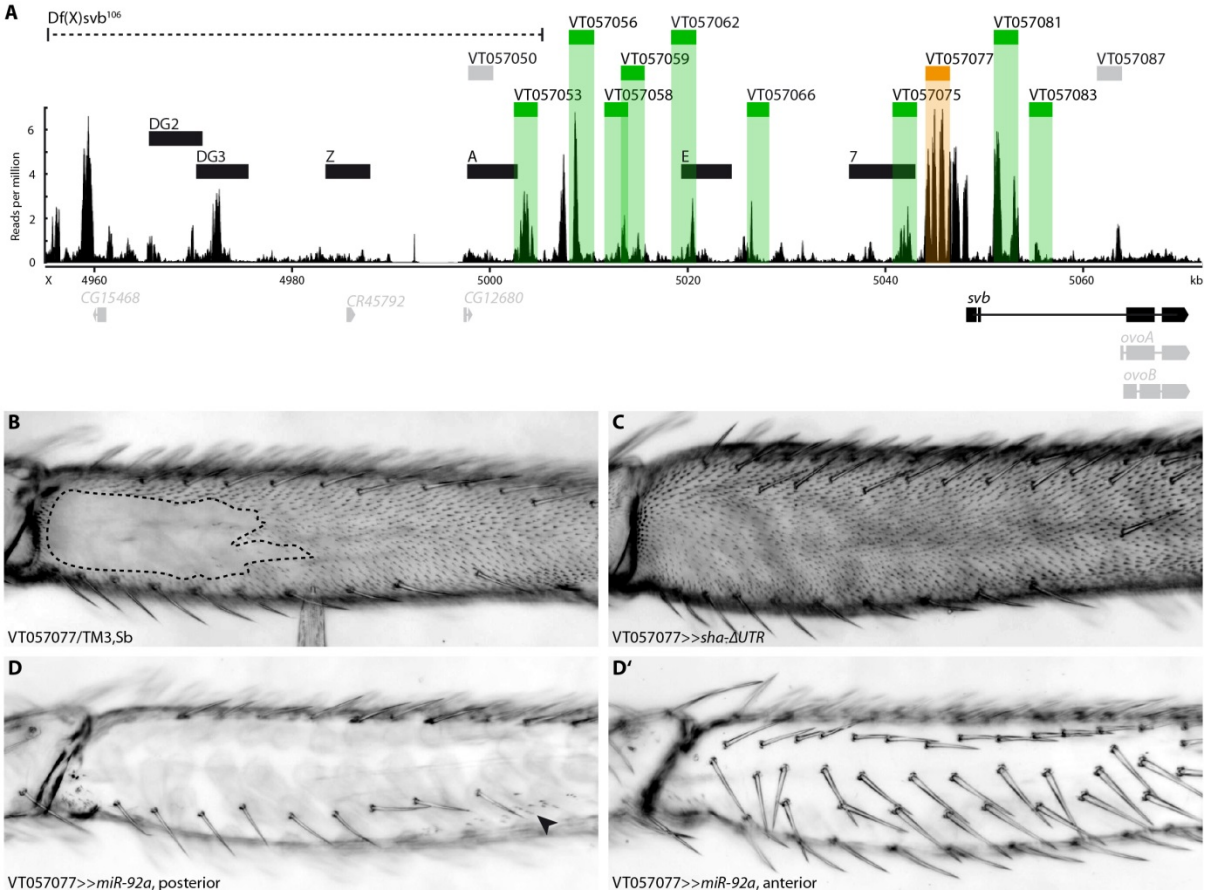

Figure 2: Enhancers of *svb*. (A) Overview of the chromatin accessibility profile after ATAC-seq at the *ovo/svb* locus. Indicated are the used deficiency (dotted line) known larval *svb* enhancers (black boxes), and tested putative enhancers (grey boxes: no expression in pupal legs, green/orange boxes: expression in pupal legs). Region VT057077 (orange) is able to drive expression during trichome formation (see B-D). The bottom panel shows expressed variants of genes at the locus (black) and genes/variants not expressed (grey). Boxes represent exons, lines represent introns. (B) VT057077 has a naked valley of intermediate size. (C) Expression of *sha*-ΔUTR under its control induces trichome formation in the naked valley. (D, D') Driving *miR-92a* with VT057077 represses trichome formation on the anterior and posterior of the second leg femur. Small patches of trichomes can sometimes still be found (arrowhead).

To further test whether the expression of any of these regions is consistent with a role in trichome formation, we used them to drive expression of the trichome repressor *miR-92a* and the trichome activator *sha*-ΔUTR (see 1). Intriguingly, driving *miR-92a* under control of one of the fragments (VT057077) caused the repression of trichomes on all legs (Fig. 2, Fig. S3) as well as on wings and halteres (Fig. S3). However, expressing *miR-92a* under control of VT057062 or VT057075 had no noticeable effect. *UAS-miR-92a* under control of some of the other fragments (VT057053, VT057056) only led to repression of trichomes in small patches along the legs consistent with the GFP expression pattern (Fig, S2, Fig. S3).

Driving *sha*-ΔUTR with VT057077 is sufficient to induce trichome formation in the naked valley (Fig. 2) and on the posterior T3 femur (Fig. S3). Driving *sha*-ΔUTR under control of any of the other nine regions did not produce any ectopic trichomes in the naked valley on T2 or on any other legs. These results indicate that VT057077 is the only tested enhancer that bears sufficient regulatory information to be involved in trichome

development throughout the second leg. Its ability to drive in the whole of the second leg, i.e. in regions which normally produce trichomes as well as in naked areas also suggests that *svb* is in fact expressed throughout the T2 leg, including the naked valley.

To test this further we examined the expression of *svb* transcripts in pupal T2 legs using in situ hybridization. However, this method produced variable results among legs and it was difficult to distinguish between signal and background in the femur (not shown). Therefore we examined the expression of a nuclear GFP inserted into a BAC containing the entire *svb* cis-regulatory region, which was previously shown to reliably capture the expression of this gene (40). We detected GFP throughout T2 legs at 24 hours after puparium formation including in the proximal region of the posterior femur (Fig. S4). This indicates that *svb* is expressed in naked valley cells that do not produce trichomes as well as more distal cells consistent with expression driven by enhancer VT057077.

miR-92a is sufficient to repress leg trichomes and acts downstream of Ubx

The above results suggest that components of the GRN for trichome production, including *svb,* are expressed in naked valley cells of the posterior T2 femur but are unable to produce trichomes. This differs to the situation in naked embryonic/larval cells and therefore might explain the differences in the genetic basis of trichome pattern evolution between these contexts. To test this further we examined the ability of genes to activate or repress leg trichomes.

It was previously shown that mutants of *miR-92a* have small naked valleys (58), which is consistent with the evolution of this locus underlying natural variation in naked valley size (1). We confirmed these findings using a double mutant for *miR-92a* and its paralogue *miR-92b* (59), which exhibits an even smaller naked valley (Fig. 3). We examined the morphology of the trichomes gained from the loss of *miR-92a* compared to the trichomes found more distally. We found that the trichomes gained were indistinguishable from the other leg trichomes (Fig. S5). This suggests that all of the genes required to generate leg trichomes are already transcribed in naked valley cells, but that *miR-92a* is sufficient to block their translation. Indeed, the extra trichomes that develop in the naked valley in the absence of *miR-92a* are dependent on *svb*, i.e. in a *svb* mutant background no trichomes are gained after a loss of *miR-92* (Fig. 3). Furthermore, these results also show that trichome repression by *Ubx* in the naked valley (41) requires *miR-92a* and that the former must play a role upstream of the latter. Thus while *Ubx* is part of the GRN for the development of trichome patterns in larvae and legs it plays opposite roles in these two contexts: in embryos *Ubx* activates *svb* to generate larval trichomes, while in legs it represses trichomes in a *miR-92a*-dependent mechanism (41, 60, 61) (Fig. 1).

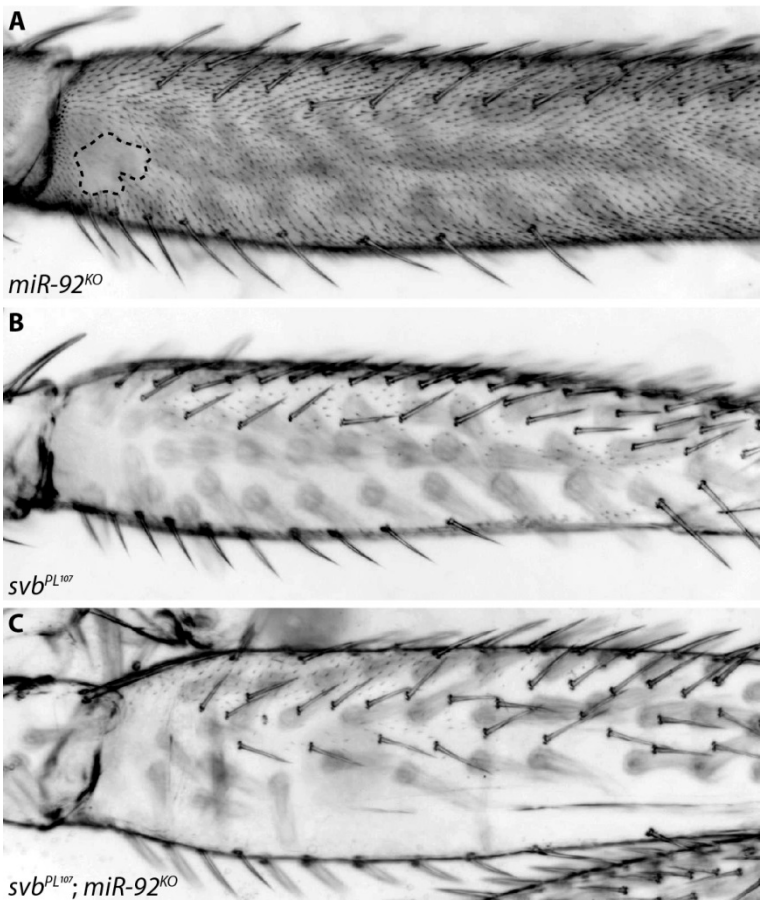

Figure 3: (A) Flies mutant for both *miR-92a* and *miR-92b* gain trichomes in the naked valley. (B) Most trichomes on the posterior T2 femur are repressed in svb^{PL107} mutant flies. (C) No trichomes are gained upon loss of *miR-92a* in a svb^{PL107} mutant background.

Svb and Sha differ in their capacities to induce trichomes in larvae and legs

It was previously shown that *miR-92a* inhibits leg trichome formation by repressing translation of the *svb* target *sha* (1). However *sha* mutants are still able to develop trichomes in larvae, albeit with abnormal morphology (30). These data suggest that there are differences in the functionality of *svb* and *sha* in larvae versus leg trichome formation and therefore we next verified and tested the capacity of *svb* and *sha* to produce larval and leg trichomes.

As previously shown (30), ectopic expression of *svb* is sufficient to induce trichome formation on normally naked larval cuticle (Fig. 4). However, we found that ectopic expression of *sha* in the same cells does not lead to the production of trichomes (Fig. 4). *svb* is also required for posterior leg trichome production (40; Figs 3, S6), but over expression of *svb* in the naked valley does not produce ectopic trichomes (Fig. 4). Over expression of *sha* on the other hand is sufficient to induce trichome development in the naked valley (1) (Fig. 4). These results show that *svb* and *sha* differ in their capacities to generate trichomes in larvae versus legs.

Svb acts as a transcriptional repressor and requires cleavage by the proteasome to become a transcriptional activator. This cleavage is induced by small proteins encoded by the *tal* locus (6, 31, 32). We therefore tested if *svb* is unable to promote trichome development in the naked valley because it is not activated in these cells. We found that expressing the constitutively active form *ovoB,* or *tal,* in naked leg cells is sufficient to induce trichome formation (Fig. 4), which is consistent with loss of *tal* in clones of leg cells resulting in the loss of trichomes (Fig. S6). Furthermore, it appears that *tal*, like *svb*, is expressed throughout the leg (Fig. S6). It follows that *svb* and *tal* are expressed in naked cells but are unable to induce trichome formation under normal conditions because of repression of *sha* by *miR-92a*. Over expression of *tal* on the other hand must be able to produce enough active Svb to result in an increase of *sha* transcription to overwhelm *miR-92a* repression.

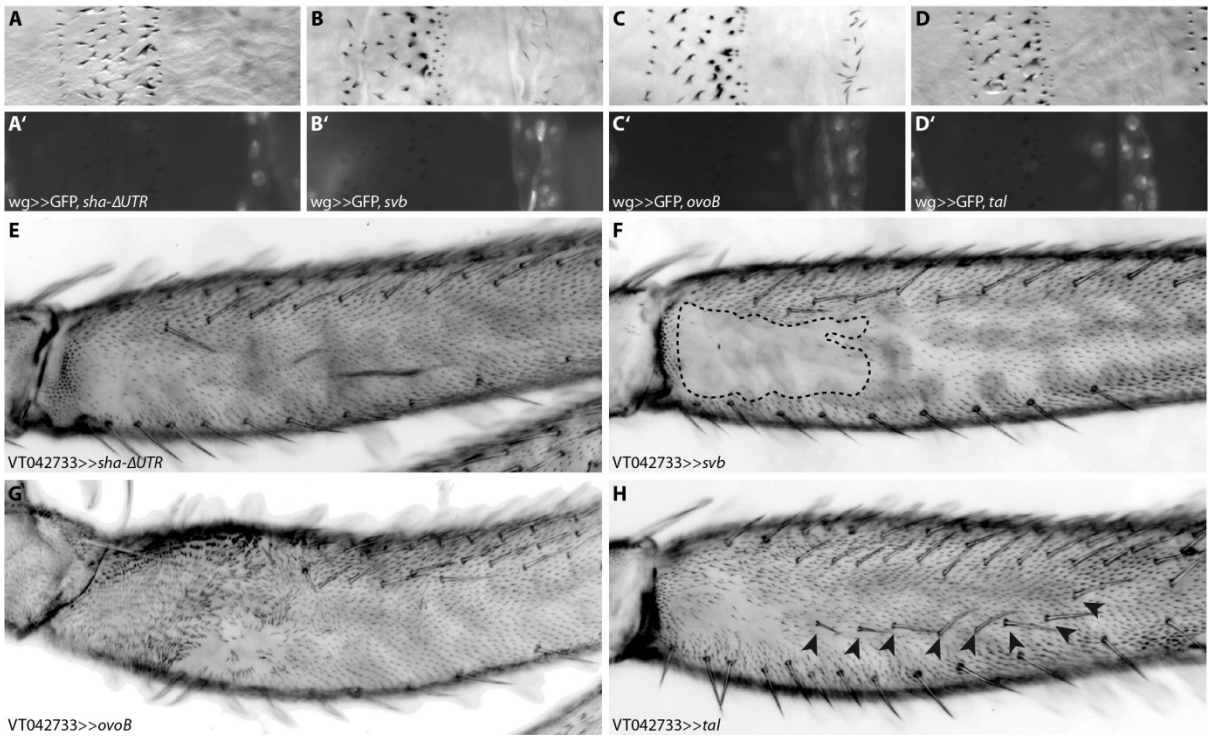

Figure 4: Ectopic trichome formation on naked cuticle. Driving *sha*-ΔUTR (A) under control of *wg*-Gal4 does not lead to ectopic trichome formation on otherwise naked larval cuticle. Driving *svb* (B) or its constitutively active variant *ovoB* (C) is sufficient to activate trichome development, but expressing only the Svb activator *tal* (D) is not. GFP was co-expressed in each case to indicate the *wg* expression domain (A'-D'). Ectopic activation of *sha*-ΔUTR in the proximal femur (E) is able to induce trichome formation, but ectopic *svb* (F) is not. Driving either *ovoB* (G) or the activator *tal* (H) leads to ectopic trichome development. Expression of *ovoB* has further effects on leg development (e.g. a bending of the proximal femur), while expression of *tal* also leads to the development of ectopic bristles on the femur (arrowheads in H).

Discussion

The GRNs for larval and leg trichome patterning differ in architecture and evolution

The causative genes and even nucleotide changes that underlie the evolution of an increasing number and range of phenotypic traits have been identified (17). An important theme that has emerged from these studies is that the convergent evolution of traits is often explained by changes in the same genes – so called evolutionary 'hotspots' (17, 62). This suggests that architecture of GRNs may influence or bias the genetic changes that underlie phenotypic changes (18, 19, 21). However, relatively little is known about the genetic basis of changes in traits in different developmental contexts and when features are gained versus lost (18).

It was shown previously that changes in *svb* underlie the convergent evolution of the loss of larval trichomes, while the gain of leg trichomes in *D. melanogaster* is instead explained by evolution of *miR-92a* (1, 13-15, 37, 38). We investigated this further by comparing the GRNs involved in both developmental contexts and examining the regulation and function of key genes.

Our results show that there are differences between the GRNs underlying the formation of larval and leg trichomes in terms of the components and the wiring used. These changes are found both in upstream genes of the GRN that help to determine where trichomes are made and in downstream genes whose products are directly involved in trichome formation (Fig. 1). The latter may also determine the differences in the fine-scale morphology of these structures on larval and leg cuticle (Fig. 1) (30).

Furthermore, while the key evolutionary switch in embryos, the gene *svb,* is also necessary for leg trichome production, this gene is not sufficient to produce leg trichomes in the naked proximal region of the T2 femur. This is because the leg trichome GRN employs *miR-92a*, which inhibits trichome production by blocking the translation of the *svb* target gene *sha*. In the legs of *D. melanogaster*, *miR-92a* acts as the evolutionary switch for trichome production, and the size of the naked valley depends on the expression of this gene (Fig. 5) (1).

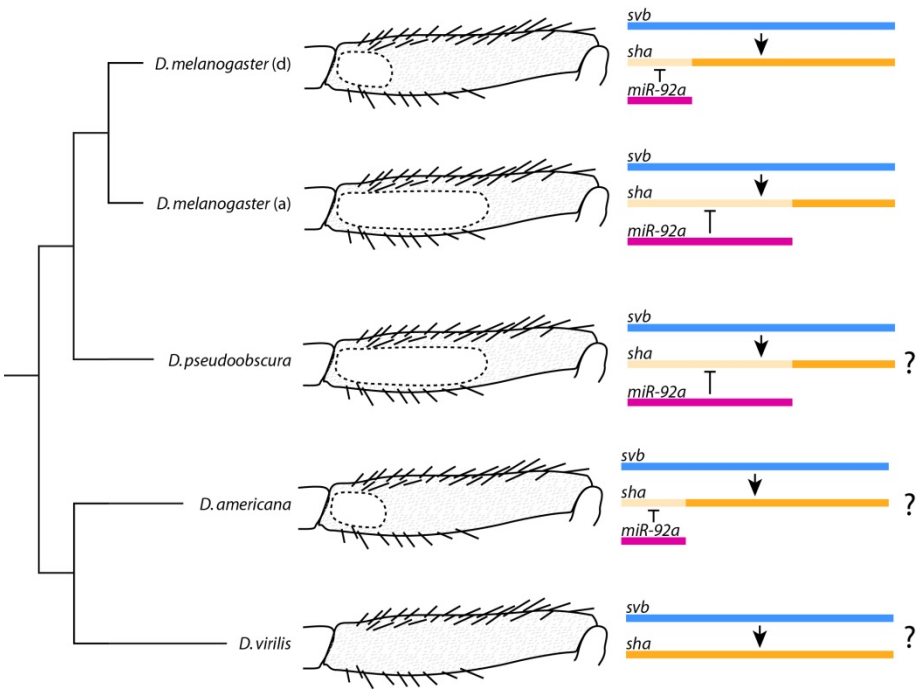

Figure 5: The size of the naked valley differs between and within species and is dependent on the level of *miR-92a* expression. Loss of *miR-92a* expression in *D. melanogaster* has led to a derived (d) smaller naked valley in some populations while the ancestral state (a) is thought to be a large naked valley like in other *melanogaster* group species (e.g. *D. pseudoobscura*). The absence of a naked valley in *D. virilis* is likely due to absence of *miR-92a* expression, while the presence of small naked valleys in other species of the *virilis* group (e.g. *D. americana*) could be explained by a gain of microRNA expression.

Interestingly, we observed that the ectopic trichomes produced by expression of *sha*-ΔUTR in the naked valley are significantly shorter than those on the rest of the leg (Fig. S5). This suggests that although *sha* is able to induce trichome formation in these cells, other genes are also required for their normal morphology. Another *svb*-target gene, *CG14395* (35), is also a strongly predicted target of *miR-92a*: its 3'UTR contains two conserved complete 8-mers corresponding to the binding site for this microRNA. We found that *CG14395* is also expressed in our leg RNA-Seq data (Table S1). Therefore it is possible that *miR-92a* represses *CG14395* and potentially other target genes in addition to *sha* to block trichome formation.

Other genetic bases for the evolution of leg trichome patterns?

In contrast to larvae, it is unlikely that mutations in *svb* can lead to evolutionary changes in legs to gain trichomes and decrease the size of the naked valley. This is because this gene (and all the other genes necessary for trichome production) is already transcribed in naked cells. In addition, a single *svb* enhancer is able to drive expression throughout the legs including the naked valley. Although other enhancer regions of this gene are able to drive some expression in patches of leg cells, none of these is naked valley-specific. This suggests that evolutionary changes to *svb* enhancers would be unlikely to only affect the naked valley. It remains possible that binding sites could evolve in this enhancer to specifically increase the Svb concentration in naked valley cells. This could overcome *miR-92a*-mediated repression of trichomes similar to experiments where *tal* and *ovoB* are over expressed in these cells, or when sponges are used to phenocopy the loss microRNAs (63). However, this does not seem to have been the preferred evolutionary route in *D. melanogaster* (1) (Fig. 5).

Our study also corroborates that *Ubx* represses leg trichomes (41) whereas it promotes larval trichome development through activation of *svb* (61). Moreover, our results indicate that *Ubx* acts upstream of *miR-92a* in legs because it is unable to repress leg trichomes in the absence of this microRNA. It is possible that Ubx even directly activates *miR-92a* since ChIP-chip data indicate that there are Ubx binding sites within the *jigr1*/*miR-92a* locus (64). Intriguingly, there is no naked valley in *D. virilis* and *Ubx* does not appear to be expressed in the second legs of this species during trichome development (41) (Fig. 5). However naked valleys are evident in other species in the *virilis* and *montana* groups and it would be interesting to determine if these differences were caused by changes in *Ubx, miR-92a* or even other loci (Fig. 5).

Evolutionary hotspots and developmental context

To the best of our knowledge, our study is the first to directly compare the GRNs underlying formation of similar structures that have evolved in different developmental contexts. Our results show that the GRNs for trichome production in larval versus leg contexts retain a core set of genes but also exhibit differences in the components used and in their wiring. These differences likely reflect changes that accumulate in GRNs during processes such as co-option (65) and developmental systems drift (66-68), although it remains possible that the changes have been selected for unknown reasons.

Importantly, we show that the differences in these GRNs may help to explain why they have evolved at different nodes to lead to the gain or loss of trichomes. This supports the suggestion that GRN architecture can influence the pathway of evolution and lead to hotspots for the convergent evolution of traits (17-19, 21). Indeed, such hotspots can also underlie phenotypic changes in different developmental contexts. For example, *yellow* underlies differences in abdominal pigmentation and wing spot pigmentation among *Drosophila* species (10, 11, 69, 70). However, we demonstrate that it cannot be assumed that evolutionary hotspots in one development context represent the nodes of evolution in a different context as a consequence of differences in GRN architecture.

Our findings also highlight that the genes that underlie the loss of features might not have the capacity to lead to the gain of the same feature. Therefore, while evolution may be predictable in particular contexts, it is very important to consider developmental context and whether a trait is lost versus gained. Indeed even when we map the genetic basis of phenotypic change to the causative genes it is important to understand the changes in the context of the wider GRN to fully appreciate how the developmental program functions and evolves. Since evolution is thought to favour changes with low pleiotropy (19, 71-74), the effects of genetic changes underlying phenotypic change should be tested more widely during development. Such an approach recently revealed that *svb* enhancers underlying differences in larval trichomes are actually also used in other contexts (40). Interestingly, *miR-92a* is employed in several roles, including self-renewal of neuroblasts (59), germline specification (58), and circadian rhythms (75). It remains to be seen if the changes in this microRNA underlying naked valley differences also have pleiotropic consequences, and therefore if natural variation in naked valley size is actually a pleiotropic outcome of selection on another aspect of *miR-92a* function.

Acknowledgements

We thank Georgina Haines-Woodhouse for technical assistance, Daniel Leite for help with bioinformatics, and members of the McGregor lab and Maike Kittelmann for comments and suggestions throughout the project. This work was funded by DFG Research Fellowships to SK (Ki 1831/1-1) and FAF (FR 3929/1-1), a BBSRC DTP studentship to ADB, grants from Ministerio de Economía y Competitividad (BFU2016-74961-P) and the Andalusian Government (BIO-396) to JLGS, and an Austrian Science Fund (FWF) Fellowship to APM (M1059-B09). RNA library preparation and sequencing were carried out by Edinburgh Genomics, The University of Edinburgh. Edinburgh Genomics is partly supported through core grants from NERC (R8/H10/56), MRC (MR/K001744/1) and BBSRC (BB/J004243/1). We thank Francois Payre (University of Toulouse), David Stern (Janelia Farm), Fen-Biao Gao (UMass Med School) and the Vienna Drosophila RNAi Center for providing fly stocks.

References

1. Arif S*, et al.* (2013) Evolution of mir-92a Underlies Natural Morphological Variation in Drosophila melanogaster. *Curr Biol* 23(6):523-528.
2. Martin A*, et al.* (2014) Multiple recent co-options of Optix associated with novel traits in adaptive butterfly wing radiations. *EvoDevo* 5(1):7.
3. Reed RD*, et al.* (2011) optix drives the repeated convergent evolution of butterfly wing pattern mimicry. *Science* 333(6046):1137-1141.
4. Chan YF*, et al.* (2010) Adaptive evolution of pelvic reduction in sticklebacks by recurrent deletion of a Pitx1 enhancer. *Science* 327(5963):302-305.
5. Colosimo PF*, et al.* (2004) The genetic architecture of parallel armor plate reduction in threespine sticklebacks. *PLoS Biol* 2(5):E109.
6. Zanet J*, et al.* (2015) Pri sORF peptides induce selective proteasome-mediated protein processing. *Science* 349(6254):1356-1358.
7. Pfeiffer BD*, et al.* (2008) Tools for neuroanatomy and neurogenetics in Drosophila. *Proc Natl Acad Sci U S A* 105(28):9715-9720.
8. Shapiro MD*, et al.* (2004) Genetic and developmental basis of evolutionary pelvic reduction in threespine sticklebacks. *Nature* 428(6984):717-723.
9. Arnoult L*, et al.* (2013) Emergence and diversification of fly pigmentation through evolution of a gene regulatory module. *Science* 339(6126):1423-1426.
10. Gompel N, Prud'homme B, Wittkopp PJ, Kassner VA, & Carroll SB (2005) Chance caught on the wing: cis-regulatory evolution and the origin of pigment patterns in Drosophila. *Nature* 433(7025):481-487.
11. Prud'homme B*, et al.* (2006) Repeated morphological evolution through cis-regulatory changes in a pleiotropic gene. *Nature* 440(7087):1050-1053.
12. Guerreiro I*, et al.* (2016) Reorganisation of Hoxd regulatory landscapes during the evolution of a snake-like body plan. *eLife* 5.
13. Frankel N*, et al.* (2011) Morphological evolution caused by many subtle-effect substitutions in regulatory DNA. *Nature* 474(7353):598-603.
14. Frankel N, Wang S, & Stern DL (2012) Conserved regulatory architecture underlies parallel genetic changes and convergent phenotypic evolution. *Proc Natl Acad Sci U S A* 109(51):20975-20979.
15. McGregor AP*, et al.* (2007) Morphological evolution through multiple cis-regulatory mutations at a single gene. *Nature* 448(7153):587-590.
16. Carroll SB (2008) Evo-devo and an expanding evolutionary synthesis: a genetic theory of morphological evolution. *Cell* 134(1):25-36.
17. Martin A & Orgogozo V (2013) The Loci of repeated evolution: a catalog of genetic hotspots of phenotypic variation. *Evolution* 67(5):1235-1250.
18. Kopp A (2009) Metamodels and phylogenetic replication: a systematic approach to the evolution of developmental pathways. *Evolution* 63(11):2771-2789.
19. Stern DL (2011) *Evolution, Development and the Predictable Genome* (Roberts and Company, Greenwood Village).
20. Stern DL & Orgogozo V (2008) The loci of evolution: how predictable is genetic evolution? *Evolution* 62(9):2155-2177.
21. Stern DL & Orgogozo V (2009) Is genetic evolution predictable? *Science* 323(5915):746-751.
22. Arif S, Kittelmann S, & McGregor AP (2015) From shavenbaby to the naked valley: trichome formation as a model for evolutionary developmental biology. *Evol Dev* 17(1):120-126.
23. Inestrosa NC, Sunkel CE, Arriagada J, Garrido J, & Godoy-Herrera R (1996) Abnormal development of the locomotor activity in yellow larvae of Drosophila: a cuticular defect? *Genetica* 97(2):205-210.
24. Goodwyn PJ, Voigt D, & Fujisaki K (2008) Skating and diving: Changes in functional morphology of the setal and microtrichial cover during ontogenesis in Aquarius paludum fabricius (Heteroptera, Gerridae). *J Morphol* 269(6):734-744.
25. Goodwyn PP, De Souza E, Fujisaki K, & Gorb S (2008) Moulding technique demonstrates the contribution of surface geometry to the super-hydrophobic properties of the surface of a water strider. *Acta biomaterialia* 4(3):766-770.
26. Ditsche-Kuru P*, et al.* (2011) Superhydrophobic surfaces of the water bug Notonecta glauca: a model for friction reduction and air retention. *Beilstein journal of nanotechnology* 2:137-144.
27. Balmert A, Florian Bohn H, Ditsche-Kuru P, & Barthlott W (2011) Dry under water: comparative morphology and functional aspects of air-retaining insect surfaces. *J Morphol* 272(4):442-451.

28. Stern DL & Frankel N (2013) The structure and evolution of cis-regulatory regions: the shavenbaby story. *Philos Trans R Soc Lond B Biol Sci* 368(1632):20130028.
29. Ren N, He B, Stone D, Kirakodu S, & Adler PN (2006) The shavenoid gene of Drosophila encodes a novel actin cytoskeleton interacting protein that promotes wing hair morphogenesis. *Genetics* 172(3):1643-1653.
30. Chanut-Delalande H, Fernandes I, Roch F, Payre F, & Plaza S (2006) Shavenbaby couples patterning to epidermal cell shape control. *PLoS Biol* 4(9):e290.
31. Kondo T*, et al.* (2010) Small peptides switch the transcriptional activity of Shavenbaby during Drosophila embryogenesis. *Science* 329(5989):336-339.
32. Galindo MI, Pueyo JI, Fouix S, Bishop SA, & Couso JP (2007) Peptides encoded by short ORFs control development and define a new eukaryotic gene family. *PLoS Biol* 5(5):e106.
33. Overton PM, Chia W, & Buescher M (2007) The Drosophila HMG-domain proteins SoxNeuro and Dichaete direct trichome formation via the activation of shavenbaby and the restriction of Wingless pathway activity. *Development* 134(15):2807-2813.
34. Rizzo NP & Bejsovec A (2017) SoxNeuro and Shavenbaby act cooperatively to shape denticles in the embryonic epidermis of Drosophila. *Development* 144(12):2248-2258.
35. Menoret D*, et al.* (2013) Genome-wide analyses of Shavenbaby target genes reveals distinct features of enhancer organization. *Genome Biol* 14(8):R86.
36. Delon I, Chanut-Delalande H, & Payre F (2003) The Ovo/Shavenbaby transcription factor specifies actin remodelling during epidermal differentiation in Drosophila. *Mech Dev* 120(7):747-758.
37. Sucena E, Delon I, Jones I, Payre F, & Stern DL (2003) Regulatory evolution of shavenbaby/ovo underlies multiple cases of morphological parallelism. *Nature* 424(6951):935-938.
38. Sucena E & Stern DL (2000) Divergence of larval morphology between Drosophila sechellia and its sibling species caused by cis-regulatory evolution of ovo/shaven-baby. *Proc Natl Acad Sci U S A* 97(9):4530-4534.
39. Preger-Ben Noon E, Davis FP, & Stern DL (2016) Evolved Repression Overcomes Enhancer Robustness. *Dev Cell* 39(5):572-584.
40. Preger-Ben Noon E*, et al.* (2017) Pleiotropy in enhancer function is encoded through diverse genetic architectures. *bioRxiv*.
41. Stern DL (1998) A role of Ultrabithorax in morphological differences between Drosophila species. *Nature* 396:463-466.
42. Schertel C, Rutishauser T, Forstemann K, & Basler K (2012) Functional characterization of Drosophila microRNAs by a novel in vivo library. *Genetics* 192(4):1543-1552.
43. Pueyo JI & Couso JP (2008) The 11-aminoacid long Tarsal-less peptides trigger a cell signal in Drosophila leg development. *Dev Biol* 324(2):192-201.
44. Halachmi N, Nachman A, & Salzberg A (2012) Visualization of proprioceptors in Drosophila larvae and pupae. *Journal of visualized experiments : JoVE* (64):e3846.
45. Gramates LS*, et al.* (2017) FlyBase at 25: looking to the future. *Nucleic Acids Res* 45(D1):D663-D671.
46. Trapnell C, Pachter L, & Salzberg SL (2009) TopHat: discovering splice junctions with RNA-Seq. *Bioinformatics* 25(9):1105-1111.
47. Trapnell C*, et al.* (2012) Differential gene and transcript expression analysis of RNA-seq experiments with TopHat and Cufflinks. *Nat Protoc* 7(3):562-578.
48. Buenrostro JD, Giresi PG, Zaba LC, Chang HY, & Greenleaf WJ (2013) Transposition of native chromatin for fast and sensitive epigenomic profiling of open chromatin, DNA-binding proteins and nucleosome position. *Nat Methods* 10(12):1213-1218.
49. Langmead B & Salzberg SL (2012) Fast gapped-read alignment with Bowtie 2. *Nat Methods* 9(4):357-359.
50. Li H*, et al.* (2009) The Sequence Alignment/Map format and SAMtools. *Bioinformatics* 25(16):2078-2079.
51. Li H (2011) A statistical framework for SNP calling, mutation discovery, association mapping and population genetical parameter estimation from sequencing data. *Bioinformatics* 27(21):2987-2993.
52. Zhang Y*, et al.* (2008) Model-based analysis of ChIP-Seq (MACS). *Genome Biol* 9(9):R137.
53. Phanstiel DH, Boyle AP, Araya CL, & Snyder MP (2014) Sushi.R: flexible, quantitative and integrative genomic visualizations for publication-quality multi-panel figures. *Bioinformatics* 30(19):2808-2810.
54. Fernandes I*, et al.* (2010) Zona pellucida domain proteins remodel the apical compartment for localized cell shape changes. *Dev Cell* 18(1):64-76.
55. Graveley BR*, et al.* (2011) The developmental transcriptome of Drosophila melanogaster. *Nature* 471(7339):473-479.
56. Buenrostro JD, Wu B, Chang HY, & Greenleaf WJ (2015) ATAC-seq: A Method for Assaying Chromatin Accessibility Genome-Wide. *Current protocols in molecular biology / edited by Frederick M. Ausubel ... [et al.]* 109:21.29.21-29.
57. Frankel N*, et al.* (2010) Phenotypic robustness conferred by apparently redundant transcriptional enhancers. *Nature* 466(7305):490-493.
58. Chen YW*, et al.* (2014) Systematic study of Drosophila microRNA functions using a collection of targeted knockout mutations. *Dev Cell* 31(6):784-800.
59. Yuva-Aydemir Y*, et al.* (2015) Downregulation of the Host Gene jigr1 by miR-92 Is Essential for Neuroblast Self-Renewal in Drosophila. *PLoS Genet* 11(5):e1005264.
60. Davis GK, Srinivasan DG, Wittkopp PJ, & Stern DL (2007) The function and regulation of Ultrabithorax in the legs of Drosophila melanogaster. *Dev Biol* 308(2):621-631.
61. Crocker J*, et al.* (2015) Low affinity binding site clusters confer hox specificity and regulatory robustness. *Cell* 160(1-2):191-203.
62. Richardson MK & Brakefield PM (2003) Developmental biology: hotspots for evolution. *Nature* 424(6951):894-895.
63. Cohen SM (2009) Use of microRNA sponges to explore tissue-specific microRNA functions in vivo. *Nat Methods* 6(12):873-874.
64. Agrawal P, Habib F, Yelagandula R, & Shashidhara LS (2011) Genome-level identification of targets of Hox

protein Ultrabithorax in Drosophila: novel mechanisms for target selection. *Scientific reports* 1:205.
65. Glassford WJ & Rebeiz M (2013) Assessing constraints on the path of regulatory sequence evolution. *Philos Trans R Soc Lond B Biol Sci* 368(1632):20130026.
66. Halfon MS (2017) Perspectives on Gene Regulatory Network Evolution. *Trends Genet* 33(7):436-447.
67. Buffry AD, Mendes CC, & McGregor AP (2016) The Functionality and Evolution of Eukaryotic Transcriptional Enhancers. *Adv Genet* 96:143-206.
68. True JR & Haag ES (2001) Developmental system drift and flexibility in evolutionary trajectories. *Evol Dev* 3(2):109-119.
69. Wittkopp PJ, Vaccaro K, & Carroll SB (2002) Evolution of yellow gene regulation and pigmentation in Drosophila. *Curr Biol* 12(18):1547-1556.
70. Jeong S, Rokas A, & Carroll SB (2006) Regulation of body pigmentation by the Abdominal-B Hox protein and its gain and loss in Drosophila evolution. *Cell* 125(7):1387-1399.
71. Nunes MD, Arif S, Schlotterer C, & McGregor AP (2013) A perspective on micro-evo-devo: progress and potential. *Genetics* 195(3):625-634.
72. True J (2003) Insect melanism: the molecules matter. *Trends in Ecology and Evolution* 18:640-647.
73. Orr HA (2000) Adaptation and the cost of complexity. *Evolution* 54(1):13-20.
74. Waxman D & Peck JR (1998) Pleiotropy and the preservation of perfection. *Science* 279(5354):1210-1213.
75. Chen X & Rosbash M (2017) MicroRNA-92a is a circadian modulator of neuronal excitability in Drosophila. *Nat Commun* 8:14707.
76. Payre F (2004) Genetic control of epidermis differentiation in Drosophila. *Int J Dev Biol* 48(2-3):207-215.
77. Stern DL (2013) The genetic causes of convergent evolution. *Nat Rev Genet* 14(11):751-764.
78. Chanut-Delalande H*, et al.* (2014) Pri peptides are mediators of ecdysone for the temporal control of development. *Nat Cell Biol* 16(11):1035-1044.

Supplementary material

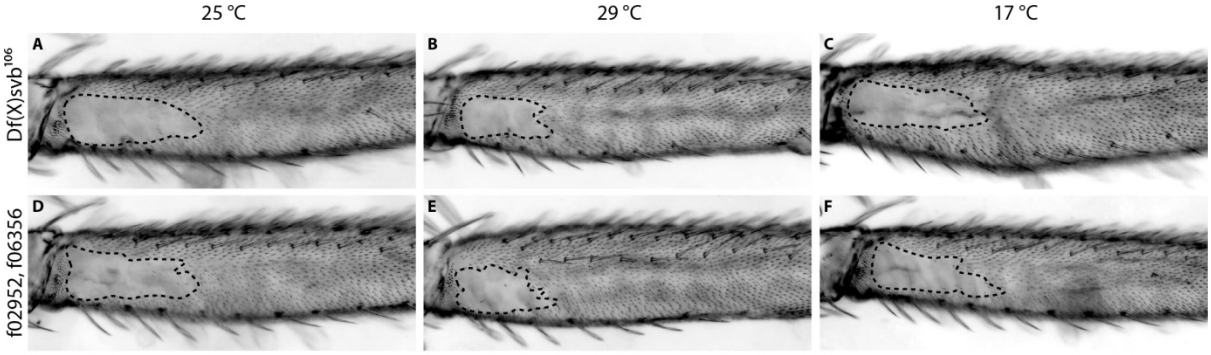

Figure S1: Naked valley size in deficiency line Df(X)106 and control line f02952,f06356 still containing both pBac insertions used to generate the deficiency (40, 56). There is no detectable difference in naked valley size or trichome density between deficiency and control flies at 25 °C, 29 °C, or 17 °C.

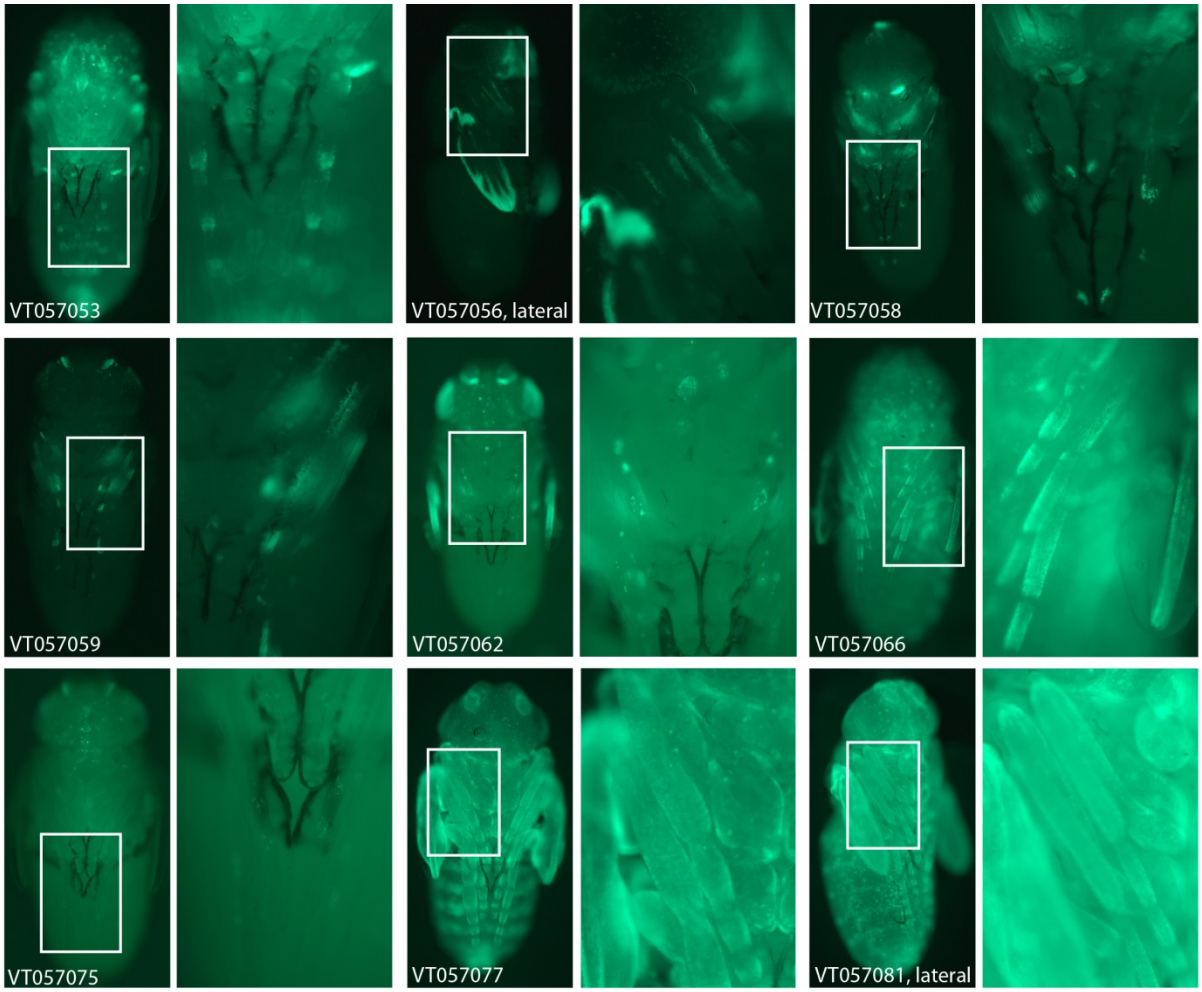

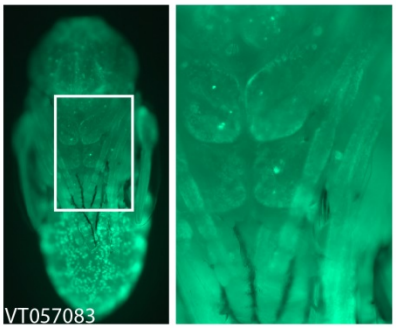

Figure S2: Expression of GFP under control of different VDRC Gal4 drivers in pupae at 22-26 hAPF.

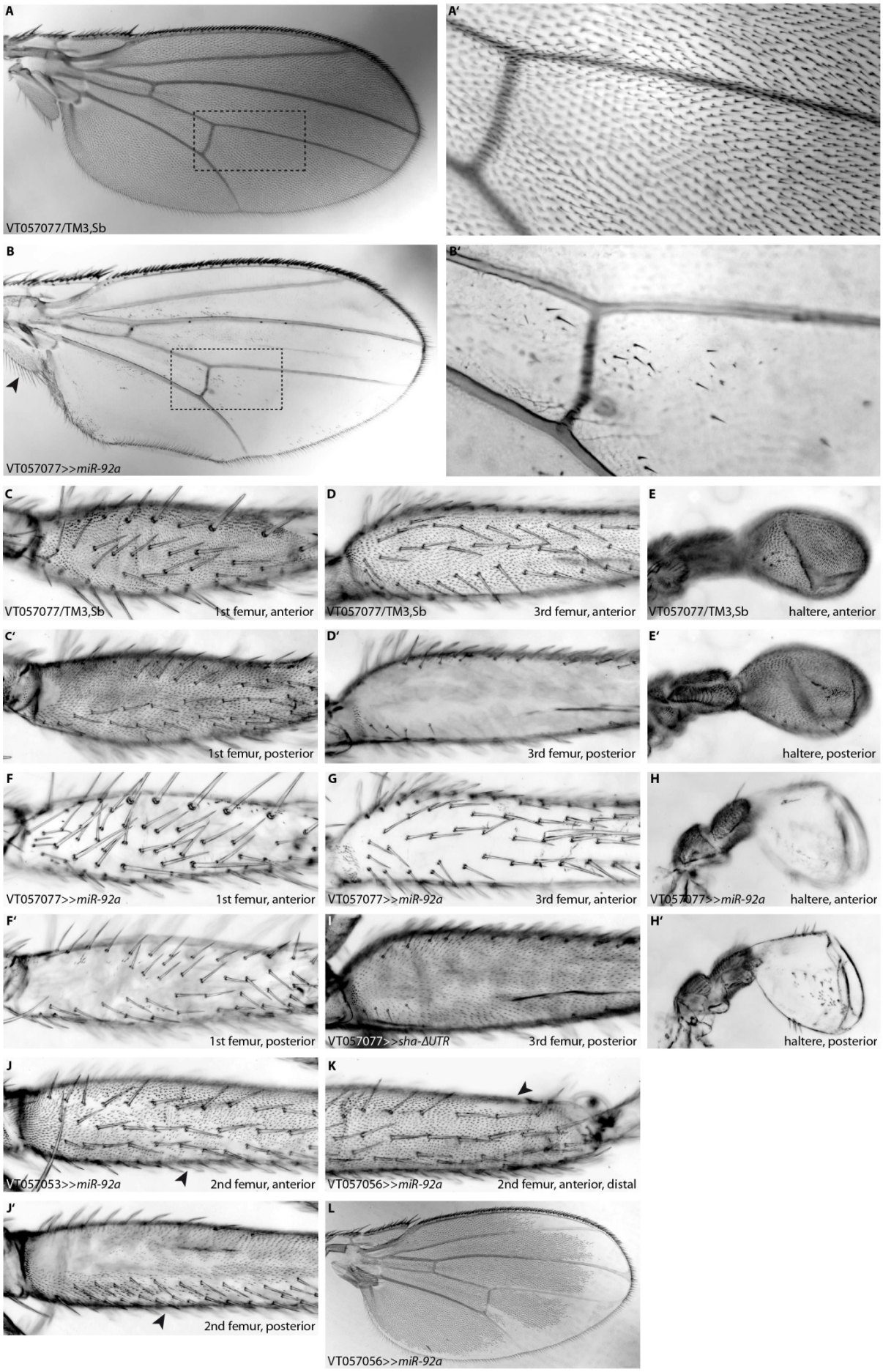
A
VT057077/TM3,Sb
A′
B
VT057077>>miR-92a
B′
C
VT057077/TM3,Sb
1st femur, anterior
D
VT057077/TM3,Sb
3rd femur, anterior
E
VT057077/TM3,Sb
haltere, anterior
C′
1st femur, posterior
D′
3rd femur, posterior
E′
haltere, posterior
F
VT057077>>miR-92a
1st femur, anterior
G
VT057077>>miR-92a
3rd femur, anterior
H
VT057077>>miR-92a
haltere, anterior
F′
1st femur, posterior
I
VT057077>>sha-ΔUTR
3rd femur, posterior
H′
haltere, posterior
J
VT057053>>miR-92a
2nd femur, anterior
K
VT057056>>miR-92a
2nd femur, anterior, distal
J′
2nd femur, posterior
L
VT057056>>miR-92a

Figure S3: Expression of *miR-92a* and *sha*-ΔUTR under control of different VT Gal4 drivers. (A, A', B, B') Trichomes on the wing are largely repressed upon expression of *miR-92a* under control of VT057077. Note that trichomes on the alula (arrowhead in B) develop normally. Also trichomes on T1 and T3 legs (C, C' D, F, F', G) and on the halteres (E, E', H, H') are repressed when *miR-92a* is driven by VT057077. (I) Driving *sha*-ΔUTR under control of VT057077 leads to ectopic formation of trichomes on the posterior T3 leg (compare to D'). (J, J') Trichomes on the ventral side of the femur are partially repressed when *miR-92a* is expressed under control of VT057053. Trichomes are repressed in a patch on the dorsal side of the distal T2 femur (K) and around the rim of the distal wing (L) after expression of *miR-92a* under control of VT057056.

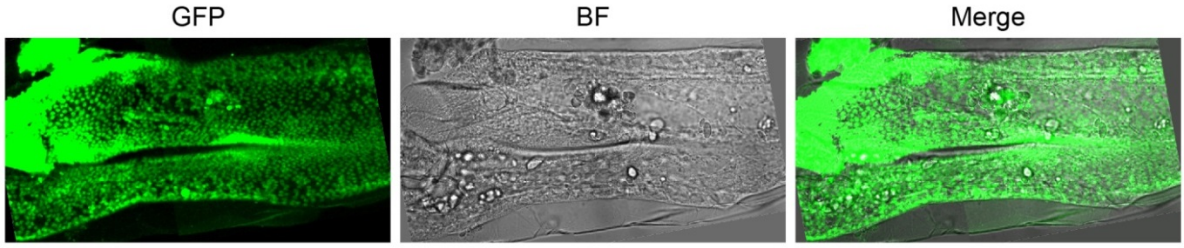

Figure S4. GFP expression driven by *svb*BAC-GFP. GFP is expressed throughout the posterior femur of a T2 leg at 24 hours APF.

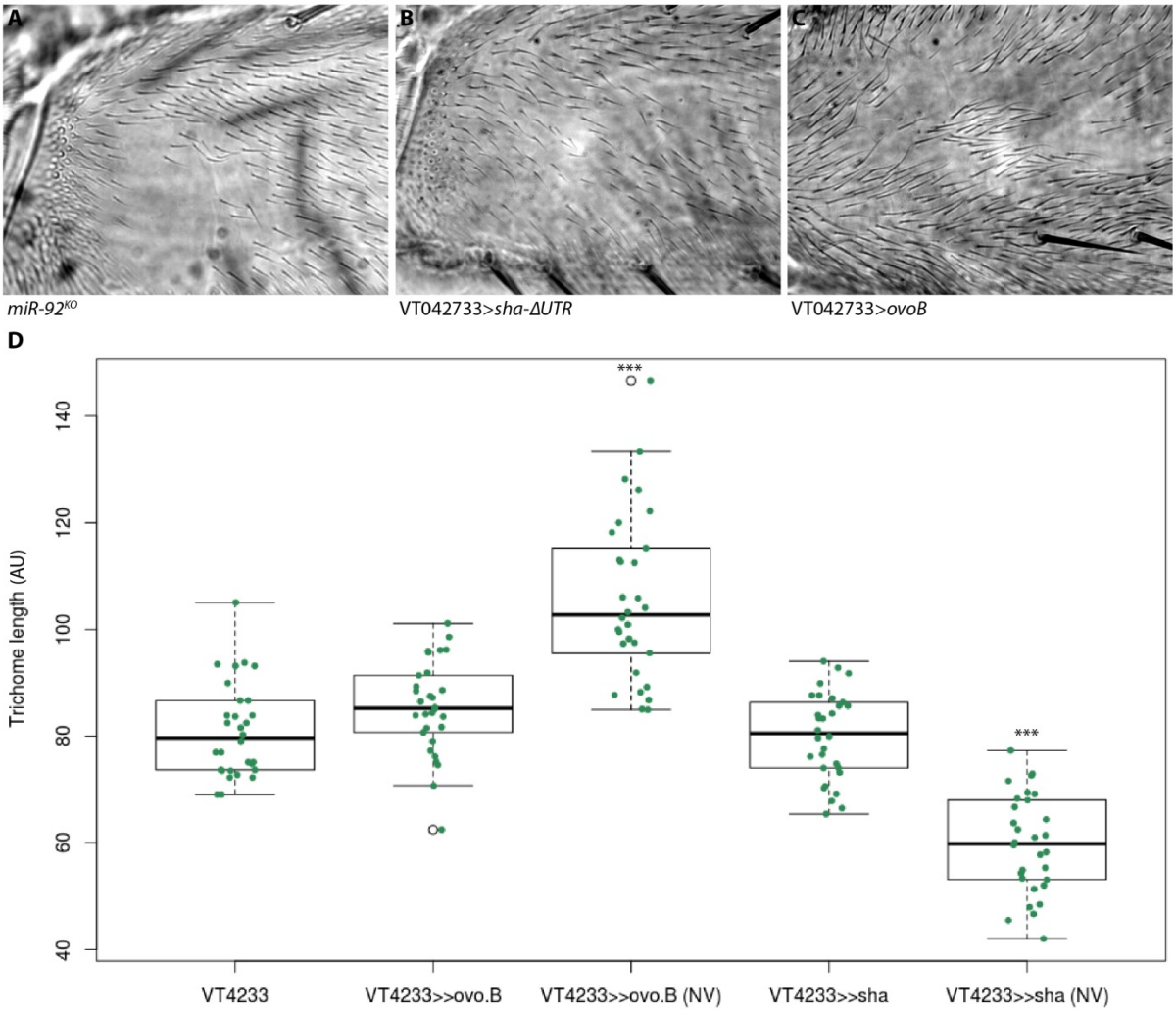

Figure S5: Trichomes gained ectopically in the naked valley have different morphologies. (A) Trichomes gained in the naked valley after loss of *miR-92a* and *miR-92b* have a similar morphology as trichomes on the more distal femur. Trichomes gained after ectopic expression of *sha*-ΔUTR (B) are significantly shorter, while trichomes developing after expression of *ovoB* (C) are significantly longer than on the remaining femur. (D) Trichomes on the more distal femur have a similar length as in the driver line (VT42733) regardless of whether *ovoB* or *sha* are expressed under its control, but trichomes gained in the naked valley are significantly longer or shorter, respectively ($p<0.001$). Tukey's multiple comparison test was used to test for significance.

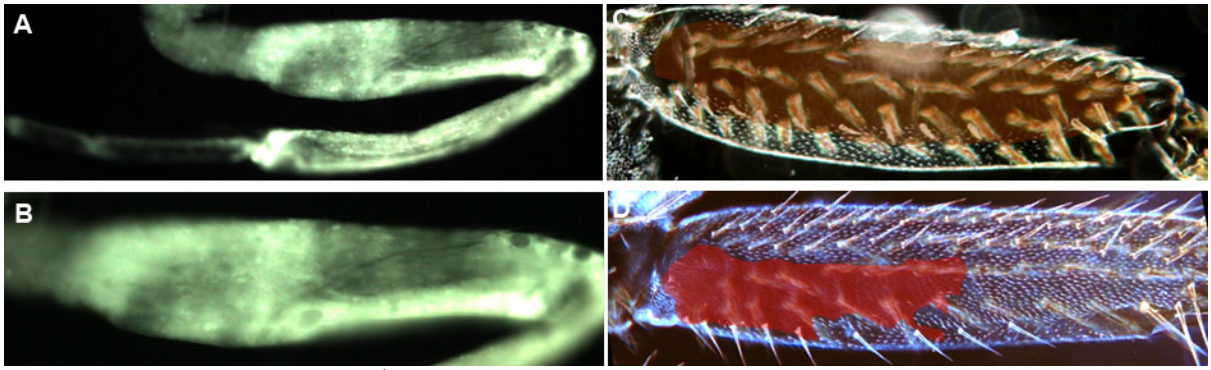

Figure S6: GFP expression driven by *tal*^{lacZ}Gal4. GFP is expressed throughout all the leg segments (A) and in the femur (B) of the second leg. Mutant clones of *tal*^{s18} (C) (brown shaded area) and *svb*^{R9} (D) (red shaded area) lack trichomes on the femur of a second leg.

Table S1: Fly strains used

Fly strain	Source, stock number (if applicable), reference
e^4, wo^1, ro^1	Bloomington #496
OregonR	N. Posnien, Goettingen, Germany
Df(X)svb^{106}	D. Stern, Janelia Farm
f02952, f06352	D. Stern, Janelia Farm
*svb*BAC-GFP	G. Sabaris and N. Frankel
VT057050	VDRC #213086
VT057053/TM3, Sb	VDRC #206968
VT057056	VDRC #207434
VT057058/TM3, Sb	VDRC #207325
VT057059	VDRC #206729
VT057062	VDRC #205634
VT057066	VDRC #205471
VT057075	VDRC #207288
VT057077/TM3, Sb	VDRC #205391
VT057081/TM3, Sb	VDRC #206590
VT057083	VDRC #206605
VT057087	VDRC #206295
VT042733	VDRC #214040
UAS-Stinger	Bloomington #65402
UAS-miR-92a	E. Lai, Memorial Sloan Kettering Cancer Center, New York, USA
UAS-sha-ΔUTR	Bloomington #32096
UAS-svb	F. Payre, Toulouse, France
UAS-ovoB	F. Payre, Toulouse, France
UAS-Ubx/TM3, Ser	Bloomington #911
UAS-tal	J.P. Couso and J.I. Pueyo-Marques
wg-Gal4	Bloomington #4918
miR-92^{KO}	F.-B. Gao, University of Massachusetts Medical School, Worcester, Massachusetts, USA
svb^{PL107}/FM0	F. Payre, Toulouse, France
y, svb^{R9}, FRT19A	F. Payre, Toulouse, France
tal^{S18}, FRT82B	J.P. Couso and J.I. Pueyo-Marques

Table S2: Expression status of upstream genes across six replicates. Values for each replicate are fragments per kilobase per million reads (FPKM). A gene was considered ON when it was expressed above 1 FPKM in the mean and in at least three replicates.

gene symbol	eworo_0513	eworo_0526	eworo_0621	OreR_0519	OreR_0525	OreR_0527	mean	status
Ubx	3.96157	8.6697	0	12.5884	5.76954	8.04185	6.50518	ON
abd-A	0.0423418	0.0299469	0.0948658	0.10903	0.0280083	0.0616258	0.06097	OFF
hh	48.4372	41.4908	77.3979	79.6048	69.4161	40.3278	59.44577	ON
wg	21.8196	28.6674	21.9651	29.4925	25.8245	30.1189	26.31467	ON
aos	18.2655	18.4636	19.9232	20.8883	22.5841	20.7375	20.14370	ON
rho	11.8349	19.492	19.9498	23.8642	23.2078	22.0168	20.06092	ON
Ser	40.9616	51.8365	45.5505	44.6192	49.2176	49.8937	47.01318	ON
spi	168.173	145.149	168.197	140.862	149.598	139.746	151.95417	ON
rl	38.4858	113.037	93.3238	160.947	115.032	197.76	119.76427	ON
Egfr	62.7771	88.9555	65.8676	93.6708	95.1875	96.9144	83.89548	ON
Dl	2.46852	16.0861	9.04308	10.5671	4.50097	18.0282	10.11566	ON
N	28.0348	59.3281	35.1895	40.5946	43.0843	50.9569	42.86470	ON
Awh	1.34117	0.720854	0.989119	1.09659	0.141291	0.895098	0.86402	OFF
ab	0.392011	1.53331	0.996614	1.50568	0	1.19534	0.93716	OFF
lin	24.6733	25.2021	85.8945	29.6993	28.4414	85.0801	46.49845	ON
D	0.927139	0.584733	0.76796	1.09142	0.504746	0.371411	0.70790	OFF
Svb/ovo	5.80587	26.3159	17.1099	23.5243	9.62429	26.0876	18.07798	ON
SoxN	1.21742	2.45478	1.67882	2.58915	1.8937	2.76856	2.10041	ON
tal	43.0835	55.6111	60.0351	54.2823	53.1971	47.5448	52.29232	ON

Table S3. Expression status of genes downstream of *svb* across six replicates. Values for each replicate are FPKM. A gene was considered ON when it was expressed above 1 FPKM in the mean and in at least three replicates. Genes are sorted alphabetically, with direct *svb* targets first, and then *svb*-independent genes.

gene symbol	eworo_0513	eworo_0526	eworo_0621	OreR_0519	OreR_0525	OreR_0527	mean	status
Actn	114.719	134.076	125.926	79.8758	139.721	90.0895	114.0679	ON
alpha-PheRS	65.2251	50.2131	52.2615	53.128	69.8619	56.3007	57.83172	ON
amd	4.57496	3.92933	7.12857	3.31174	3.85807	3.28882	4.348582	ON
bw	0	0	0	0	0	0	0	OFF
Cbs	125.966	91.8723	107.167	75.4674	77.1956	56.0348	88.95052	ON
Cda5	2.54286	5.4795	0	5.34188	2.40208	4.55044	3.386127	ON
CG10175	2.25043	1.89945	2.03885	3.29086	2.85577	3.15731	2.582112	ON
CG10585	13.7878	10.6104	9.86908	10.6586	9.47958	10.5432	10.82478	ON
CG10591	0.0773772	0.226752	0.0971719	0.142104	0.261717	0.29442	0.183257	OFF
CG10932	53.308	41.6198	48.5514	25.044	27.1913	22.4895	36.36733	ON
CG11127	50.5897	30.3484	44.7561	37.4851	37.4167	32.6071	38.86718	ON
CG11200	15.7764	12.4699	13.3267	32.4538	20.1862	15.1259	18.22315	ON
CG11227	0.00786661	0	0.00660359	0	0.00761279	0	0.00368	OFF
CG11771	20.8243	17.0666	17.3107	20.827	18.8528	18.2254	18.85113	ON
CG11786	0.058093	0.39173	646.692	338.726	217.763	332.913	256.0906	ON
CG11836	0	0	0	0	0	7.67286	1.27881	OFF
CG12009	2.76546	3.11291	1.13736	1.23102	0.906483	1.67122	1.804076	ON
CG12017	0.750667	0.686161	1.38064	1.11104	0.95148	0.570994	0.908497	OFF
CG12075	40.4702	67.1381	51.9768	44.1805	42.5097	49.3439	49.26987	ON
CG1273	69.499	114.324	79.7305	100.741	98.4604	112.244	95.83315	ON
CG12814	56.7863	54.7107	59.9299	61.7902	63.8232	71.6654	61.45095	ON
CG13082	789.235	680.163	782.007	992.834	1360.66	748.171	892.1783	ON
CG13365	90.3355	42.3231	52.6198	40.9699	37.6912	0	43.98992	ON
CG13585	240.934	208.438	300.123	157.522	270.525	162.953	223.4158	ON
CG13616	0	0	0.0748567	0	0	0	0.012476	OFF
CG13627	8.05173	101.493	116.253	6.62745	6.93071	5.4723	40.8047	ON
CG13630	64.0417	53.9662	64.1155	45.3507	54.3647	46.3505	54.69822	ON
CG13698	48.8606	51.9603	44.1333	48.851	57.9348	49.5516	50.21527	ON
CG14356	0.0608778	0.0820677	0	0.127411	0.205633	0.23122	0.117868	OFF
CG14395	18.3217	19.7032	16.9092	12.7615	15.0297	13.4715	16.0328	ON
CG14756	0	0.0723682	0	0	0	0	0.012061	OFF
CG15005	0	0	2.53844	0	0	0	0.423073	OFF
CG15022	0	0.0176719	0	0	0	0	0.002945	OFF
CG15239	3.38957	3.46688	5.07793	3.15966	2.75627	2.27126	3.353595	ON
CG15506	0.675969	1.01355	0.92938	1.39249	1.09823	1.20634	1.05266	ON
CG15743	47.9489	38.9401	43.2973	37.073	37.7301	32.4783	39.57795	ON
CG1632	32.7086	12.3509	13.726	38.6845	12.9345	12.8908	20.54922	ON
CG16798	111.672	99.3248	110.989	88.25	99.1658	82.4625	98.64402	ON
CG17211	41.0175	67.0927	36.8046	56.6238	46.3947	57.6899	50.9372	ON
CG17672	121.01	90.2647	117.963	84.8002	88.2056	79.9865	97.03833	ON
CG18249	2.7265	2.13373	2.67071	1.86121	2.06159	1.9896	2.240557	ON
CG2016	135.41	91.3952	117.936	92.6503	89.4503	85.6648	102.0844	ON
CG2663	28.9773	26.1779	36.6191	18.187	21.0098	13.5315	24.08377	ON
CG30283	3.67648	2.85238	6.53419	4.9813	0	6.88943	4.15563	ON
CG30423	385.633	320.733	461.044	319.318	388.897	309.217	364.1403	ON
CG31559	22.8125	20.8558	22.3687	18.9573	24.4559	16.8954	21.0576	ON
CG31717	38.8318	27.3444	44.2569	28.8833	31.874	29.572	33.4604	ON
CG32039	29.4335	0	31.552	0	0	23.2652	14.04178	ON
CG32354	56.2021	54.96	75.7622	56.1783	52.6412	49.276	57.5033	ON
CG32694	0.083158	0.232417	0.291798	0.270697	0.0844864	0.142688	0.184207	OFF
CG34007	1.93069	1.7739	2.40376	2.65903	2.84065	2.20887	2.302817	ON
CG3831	5.19143	4.61077	4.62361	5.37446	0	5.31123	4.18525	ON
CG3842	117.028	94.8283	126.555	97.4519	110.916	109.572	109.3919	ON
CG4065	31.3795	29.2324	28.264	26.2256	29.2558	22.907	27.87738	ON

CG42331	0	0	0	0	0	0	0	OFF
CG43366	10.3573	34.2963	19.5743	35.7459	17.1429	36.3771	25.5823	ON
CG4666	24.2454	20.7701	23.7922	11.0269	18.1388	9.71517	17.9481	ON
CG4678	53.8515	50.2398	87.4828	41.8179	47.3087	35.054	52.62578	ON
CG4686	73.1947	52.2901	82.7246	31.0654	67.2572	57.2672	60.6332	ON
CG4702	12.7822	11.1633	52.7332	16.4811	9.62498	7.33159	18.35273	ON
CG4822	45.1305	45.6507	45.7504	34.4805	45.2011	38.2563	42.41158	ON
CG4914	80.6235	133.828	162.608	179.588	78.9926	66.0401	116.9467	ON
CG5039	12.5576	11.0732	15.0445	0	5.3294	0	7.334117	ON
CG5171	27.4673	26.2825	35.0987	12.2601	12.8842	14.5363	21.42152	ON
CG5525	279.456	211.383	214.93	277.97	233.358	236.676	242.2955	ON
CG5742	10.3207	0	10.4358	122.878	12.5385	11.6493	27.97038	ON
CG6180	232.136	169.083	220.017	184.106	232.821	164.942	200.5175	ON
CG6415	0.113337	0.146129	0.624001	0.0510158	0.109569	0.035222	0.179879	OFF
CG6785	399.068	468.252	0	564.611	359.464	426.6	369.6658	ON
CG7173	1.57305	1.64877	1.79773	7.3361	7.604	6.82406	4.463952	ON
CG7840	0	53.7831	60.4179	59.7266	0	62.4257	39.39222	ON
CG7860	200.265	207.832	284.758	98.5235	124.486	98.6631	169.0879	ON
CG8112	16.5228	16.3278	15.6203	12.4226	10.5149	7.16534	13.09562	ON
CG8213	0.415967	0.763361	0.767078	0.723779	0.61271	0.567572	0.641745	OFF
CG8303	17.6132	16.9785	20.4947	14.5166	16.7612	15.2031	16.92788	ON
CG8306	112.156	91.0755	100.432	0	98.8701	79.602	80.35593	ON
CG8386	188.582	176.146	190.839	0	155.296	0	118.4772	ON
CG8420	43.8504	36.7529	139.83	38.8997	32.7016	0	48.67243	ON
CG9095	6.37894	10.148	8.40065	7.86694	7.43329	6.88766	7.85258	ON
CG9175	35.2654	31.706	31.867	32.0753	36.2534	28.4553	32.60373	ON
CG9184	0	0	1.30409	0	0	0	0.217348	OFF
CG9205	121.424	117.662	122.934	81.4312	89.8938	0	88.89083	ON
CG9356	36.2442	28.6182	34.6581	31.6091	32.2473	28.1021	31.91317	ON
CG9503	52.2362	57.489	54.4764	55.956	65.9219	62.8874	58.16115	ON
CG9514	0.0966563	0.191407	0.273956	0.108145	0.0935585	0.197453	0.160196	OFF
CG9519	0.00946666	0.0770503	0.0635503	55.956	0.0549566	0.113391	9.379069	OFF
CG9689	463.6	365.898	481.107	310.178	286.541	319.219	371.0905	ON
cher	8.26661	12.6198	64.6546	14.1557	15.1979	15.2284	21.68717	ON
ChLD3	16.5881	16.0087	14.8148	8.57203	10.4764	7.69797	12.35967	ON
CHOp24	237.993	173.961	234.61	178.8	188.569	174.078	198.0018	ON
Cpr11A	0	0.0274356	0.0382004	0.015963	0.0146914	0.11571	0.035333	OFF
crok	147.871	108.314	150.669	114.126	125.635	117.95	127.4275	ON
Cyp301a1	2.96024	2.42004	2.8454	6.16276	4.51657	3.75397	3.776497	ON
cyr	0	0	6.53292	37.388	69.8619	43.1376	26.1534	ON
cysu	3.11811	3.82415	3.36382	3.7678	3.30056	3.8409	3.53589	ON
dsx-c73A	100.249	114.453	103.261	104.411	113.783	99.7149	105.9787	ON
dyl	0.322737	0.241284	0.523761	0.267031	0.247438	0.183728	0.297663	OFF
ect	58.7089	56.6778	57.4419	50.202	44.8657	42.0081	51.65073	ON
f	0	0	10.0568	0	3.39035	3.33063	2.796297	ON
Fib	48.147	59.0667	43.8283	34.5798	57.8052	40.835	47.377	ON
fw	13.4289	13.2683	14.0368	15.7273	15.1042	13.8398	14.23422	ON
GILT3	44.8446	33.2886	38.1122	30.1016	58.6553	27.974	38.82938	ON
Gmap	11.5972	11.0572	12.1616	10.4953	14.9159	10.1779	11.73418	ON
Gtp-bp	131.585	97.6869	113.828	103.789	107.39	90.4687	107.4579	ON
hll	14.8125	13.0502	12.1408	11.9919	5.48823	6.24292	10.62109	ON
Hmgs	0	0	0	0	0	0	0	OFF
Hr3	0.0751861	0.398092	0.978592	0.815259	0.144463	0.78028	0.531979	OFF
ImpE1	5.70185	12.8599	8.63181	10.8993	8.51564	11.6175	9.704333	ON
kar	11.3006	82.5887	86.123	90.7659	92.1296	80.5511	73.90982	ON
kkv	59.1943	70.9463	60.1457	84.5062	80.6819	93.2022	74.77943	ON
Lip4	2.31355	2.06452	2.73079	2.77734	2.57632	2.74969	2.535368	ON
m	2.90568	61.8022	51.7087	4.2815	3.27869	1.94652	20.98722	ON

mas	19.0467	23.2224	20.8718	21.1666	23.7837	22.6603	21.79192	ON
mey,nyo	330.519	371.461	424.226	385.587	360.347	291.419	360.5932	ON
mRpL45	27.1025	22.6185	24.5445	26.3427	24.8449	24.6379	25.01517	ON
mRpL46	0	25.4484	45.9734	0	0	22.5604	15.6637	ON
mRpL47	48.022	34.31	54.1329	47.2721	0	32.4186	36.02593	ON
mRpL51	55.6169	37.4157	50.836	39.3414	38.5238	32.4546	42.36473	ON
mwh	34.467	39.1108	34.836	36.6654	44.3577	30.7105	36.69123	ON
neo	466.786	503.336	526.854	498.877	541.726	434.362	495.3235	ON
Nf-YA	56.163	51.6492	56.5873	51.049	54.124	49.4356	53.16802	ON
NimB3	18.4233	7.97715	29.147	15.7306	35.2267	13.4421	19.99114	ON
Obp99c	381.077	243.22	376.128	323.878	443.298	270.36	339.6602	ON
Orct	21.5917	21.322	20.5909	25.9658	28.8937	21.9706	23.38912	ON
Osi24	10.9463	8.58122	8.76095	8.63532	9.42421	6.68231	8.838385	ON
Past1	71.5619	60.3347	71.5275	60.3859	67.0434	61.9464	65.46663	ON
Peritrophin-A	0	0	43.1015	0	0	0	7.183583	OFF
PH4alphaEFB	60.8201	63.684	64.734	84.1358	69.2521	86.1595	71.46425	ON
PH4alphaSG1	0	0	0.0192157	0.0120458	0	0	0.00521	OFF
pk	94.0105	117.34	102.255	106.523	119.974	119.117	109.8699	ON
PKD	48.1294	44.3817	48.1013	53.6297	49.7884	50.8983	49.1548	ON
PMP34	27.3652	18.492	24.0645	22.0861	24.5499	19.0594	22.60285	ON
Prosalpha4	251.597	186.225	228.471	189.676	198.063	181.542	205.929	ON
prtp	107.234	99.9868	93.6789	101.629	105.267	78.3361	97.68863	ON
PTPMT1	0	0	153.492	0	0	0	25.582	OFF
pwn	64.7159	63.013	56.5957	49.7824	53.1783	53.7628	56.84135	ON
Rab23	67.2992	84.4214	75.5584	79.6302	78.3834	82.621	77.9856	ON
Rcd6	46.5085	12.8551	12.5079	13.9477	13.6877	14.1306	18.93958	ON
Rpb8	85.8704	71.417	73.7988	56.3209	71.8779	67.4894	71.12907	ON
RpS1	3738.71	2552.82	3677.49	2963.73	3102.94	2159.79	3032.58	ON
rt	11.2374	12.8532	12.4943	11.0042	12.78	10.4015	11.7951	ON
SCOT	33.4385	28.5025	32.0056	32.951	34.0308	30.7218	31.9417	ON
scu	261.603	194.024	228.717	193.32	213.628	174.052	210.8907	ON
Sec23	148.288	127.762	117.846	99.4197	99.5781	83.0698	112.6606	ON
sha	13.1666	20.8565	14.7783	17.7945	20.644	18.6642	17.65068	ON
Smn	156.113	121.726	146.473	125.084	129.857	110.415	131.6113	ON
sn	122.09	163.963	156.135	163.425	188.398	172.06	161.0118	ON
snRNP-U1-C	153.345	113.292	117.041	117.567	132.109	113.779	124.5222	ON
Sox21b	0.206853	0.347864	0.313827	0.425909	0.165713	0.302994	0.29386	OFF
Spn88Ea	250.737	189.721	241.769	252.184	242.505	199.181	229.3495	ON
St4	36.2816	0	0	28.7292	37.237	36.5728	23.13677	ON
Tb	0	0	0	0	0	0	0	OFF
T-cp1	236.959	177.899	181.729	230.272	198.583	203.145	204.7645	ON
Tg	6.25973	0	0	12.4413	8.69108	0	4.565352	ON
TRAM	233.843	182.561	212.736	183.359	197.489	176.451	197.7398	ON
tw	85.765	234.955	131.417	155.404	147.636	151.059	151.0393	ON
tyn	483.102	707.361	728.085	779.011	628.443	673.489	666.5818	ON
WASp	9.49092	13.5541	10.0474	11.2016	12.6972	13.2155	11.70112	ON
y	0.0377862	0.239204	0.28537	0.258411	0.658079	0.411456	0.315051	OFF
ZnT86D	0	0	0	33.5449	0	3303.36	556.1508	OFF
zye	0.00517209	0.0117175	0.0282556	0.0547331	0.0225379	0.0789357	0.033559	OFF
Cad96Ca	36.9979	38.084	32.7502	36.586	41.221	39.4514	37.51508	ON
CadN	1.67753	9.37694	3.59994	7.92133	3.92399	13.652	6.691955	ON
CG13699	0.0839789	0.111837	0.0497955	0.182121	0.219984	0.172259	0.136663	OFF
CG14626	0.282863	0.242677	0.50977	0.252658	0.246175	0.215442	0.291598	OFF
CG14830	35.7731	31.9571	38.0452	29.9373	36.1813	34.3927	34.38112	ON
CG15080	0	1.91988	1.04509	1.24787	0.383263	1.04785	0.940659	OFF
CG15282	0.693707	1.04047	0.517227	4.97646	2.37979	2.3599	1.994592	ON
CG15370	0.0486616	0.0292789	0.0135899	0.0170362	0.0940876	0.0529292	0.042597	OFF
CG15818	0	0.0137764	0.0127879	0	0	0	0.004427	OFF

CG16885	6.16761	5.82283	3.65816	8.1881	7.98848	5.48829	6.218912	ON
CG17562	0	0	0.00982245	0	0.0226568	0	0.005413	OFF
CG17781	0	0	0	0.013842	0.0254716	0	0.006552	OFF
CG17786	4.32716	6.00346	4.88876	7.42957	6.97575	0	4.93745	ON
CG2767	220.922	172.319	202.134	146.097	211.597	141.896	182.4942	ON
CG30101	34.0223	26.1544	34.2473	44.9923	49.8226	45.0484	39.04788	ON
CG32137	23.0734	25.4202	23.4416	26.1435	26.2974	26.8886	25.21078	ON
CG4386	38.7357	38.7107	42.4376	41.1092	42.8058	5107.41	885.2015	ON
CG5065	1.26867	4.88362	3.11681	3.44467	2.99655	3.62154	3.221977	ON
CG5756	0.334791	0	0	6.62854	0	0	1.160555	OFF
CG8170	1.17855	1.14604	0.866938	1.18104	1.73408	1.00192	1.184761	ON
CG8239	30.696	20.9931	213.663	27.5234	25.3237	24.9467	57.19098	ON
CG9990	26.3899	35.7401	24.7928	39.3898	31.7615	29.7955	31.3116	ON
Clect27	8.38484	5.95054	8.23875	16.4987	4.25419	7.55904	8.48101	ON
Dhit,grh	24.3279	81.73	47.5006	62.2465	35.9118	80.8172	55.42233	ON
dpy	4.01742	17.8891	6.26019	24.1336	19.6861	21.2527	15.53985	ON
jbug	78.3867	89.5062	78.2843	80.3998	88.5427	89.2314	84.05852	ON
knrl	1.80585	3.23872	11.9038	11.3573	2.99541	10.7656	7.011113	ON
kst	9.77018	21.1924	11.2331	20.1917	18.9821	22.0984	17.24465	ON
Obp83g	48.0961	39.7109	51.1382	46.1496	57.0253	86.2937	54.73563	ON
Osi17	0.194516	0.271721	0.411844	0.275106	0.237935	0.0726668	0.243965	OFF
pio	451.16	442.822	468.045	495.338	473.575	388.536	453.246	ON
pot	152.199	195.386	169.613	186.715	210.004	202.709	186.1043	ON
qua	17.6662	16.844	17.6516	20.6613	18.0253	17.222	18.01173	ON
RhoGEF64C	8.93645	13.9511	11.1465	12.0023	11.4772	11.1467	11.44338	ON
spir	5.82371	42.9094	9.59011	16.0133	12.1572	15.4921	16.99764	ON
spz6	354.35	264.941	312.567	239.511	236.375	191.545	266.5482	ON
TwdlG	0.0208529	0.0560308	0.0520836	0.0744966	0.0256886	0.118956	0.058018	OFF
vri	18.3233	18.3911	16.406	18.493	16.8458	21.1298	18.26483	ON
Wdr62	10.8693	20.9829	14.1998	18.3395	16.688	20.7204	16.96665	ON
wus	47.9685	46.4703	50.6354	47.6976	46.9848	38.4373	46.36565	ON
yellow-b	9.54555	47.6266	41.0385	24.6259	77.35	37.3698	39.59273	ON
yellow-d	0	0	0	0	0	0	0	OFF
yellow-e3	0	0.138	0.0896688	0.0160587	0.0295593	1.36459	0.272979	OFF

Table S4. Expression status of genes expressed in legs at 20-28 h APF but not in embryos at 12-16 h. Values for each replicate are FPKM. Genes are sorted alphabetically. Genes with a GO term indicating a potential function in trichome development are highlighted in green, (putative) TFs are highlighted blue.

gene symbol	eworo_0513	eworo_0526	eworo_0621	OreR_0519	OreR_0525	OreR_0527	mean
Act88F	3.29865	0	3.50138	28.1402	0	20.0522	9.165405
alpha-Est3	25.8985	16.9575	28.2401	0	15.2695	11.9219	16.38125
AttD	7.79611	6.65226	13.3249	2.60308	3.36677	2.33727	6.013398
bab1	0	58.834	44.9851	65.6321	26.3831	57.5493	42.2306
CecA1,CecC	37.4286	36.4183	84.8996	56.3722	114.515	66.3924	66.00435
CecB	7.59773	5.99303	21.9433	7.60458	20.4111	10.9058	12.40926
CG10680	15.7442	54.5127	18.6927	9.58	12.3531	11.2838	20.36108
CG11570	31.8734	0.616545	28.2301	14.1588	17.3925	4.90312	16.19574
CG11835	84.445	106.401	65.7847	90.2042	99.458	94.3389	90.1053
CG11852	45.5132	28.3032	37.0774	104.438	26.6469	41.2139	47.19877
CG11951	707.749	689.581	663.16	46.8505	57.7364	49.9692	369.1744
CG13056	343.665	216.687	349.47	490.72	428.366	461.625	381.7555
CG13071	120.508	87.07	108.55	67.5896	82.6183	74.828	90.19398
CG13081	548.351	511.585	666.319	992.834	1360.66	748.171	804.6533
CG13117	33.9055	28.3911	47.1919	44.5514	51.4788	44.5373	41.676
CG13578	7.98558	5.86325	10.5884	4.3702	6.05468	3.70205	6.42736
CG13639	87.9683	72.0471	89.5908	11.3932	16.7594	11.2897	48.17475
CG13670	5.12972	4.80087	9.86033	2.75931	3.05119	2.85919	4.743435
CG13728	3.50574	3.6655	3.62959	4.52713	5.12943	3.71963	4.029503
CG14218	7.85701	6.20509	5.91408	3.94365	7.32822	5.20319	6.075207
CG14244	54.1839	1.97091	44.4221	11.5972	24.2578	4.48335	23.48588
CG14324	9.8101	7.92256	7.47041	14.2121	10.7687	9.10218	9.881008
CG14915	53.5769	43.2026	62.0818	19.0847	30.3174	24.8268	38.84837
CG14984	436.256	311.74	436.673	224.059	253.799	196.487	309.8357
CG15322	4.32481	4.46658	3.7982	6.34104	5.82994	5.51744	5.046335
CG15369	14.5023	14.672	29.6753	5.8298	14.5365	12.2595	15.2459
CG16704	22.276	18.3241	47.3581	12.19	21.0557	23.2327	24.07277
CG16772	43.5883	54.5127	50.9932	49.4561	63.5897	49.2965	51.90608
CG17108	21.1991	21.018	22.0733	18.5364	28.4177	15.491	21.12258
CG17490	10.2862	0	15.4787	0	10.7762	21.105	9.607683
CG18067	5.50749	4.5619	14.5138	8.82331	8.21277	7.37098	8.165042
CG18636	3.22885	2.01463	3.08878	2.67966	2.3404	1.97979	2.555352
CG18673	19.9897	33.6341	49.2484	10.2766	6.23314	4.91689	20.71647
CG30026	2.40587	2.33293	3.9322	3.19201	4.51678	4.93446	3.552375
CG30049	2.03899	1.97149	1.61308	1.69843	4.0601	1.64334	2.170905
CG33199	62.5478	57.7896	61.5908	51.1593	57.3073	53.6942	57.34817
CG34057	79.0638	67.7473	79.4532	30.6501	28.8169	40.8969	54.43803
CG34107	2.69562	2.73159	3.40173	2.81458	3.05075	3.0481	2.957062
CG34193	5130	4823.28	4706.8	2.8359	3.0982	4349.17	3169.197
CG34247	22107.2	12574.1	22252.8	10532.5	10301.4	8410.54	14363.09
CG3649	83.7357	67.7914	76.8634	71.612	77.7473	67.4091	74.19315
CG42231	47.3877	57.7811	47.6137	36.6793	22.3092	18.5905	38.39358
CG42711	7.5451	6.76021	7.13216	4.23869	5.73198	6.12058	6.254787
CG42792	138.857	103.88	179.581	52.9331	63.2961	34.8385	95.56428
CG42867,CR42868	23.3684	17.4352	0	16.854	0	23.3342	13.49863
CG43060	23.4106	16.9105	30.122	19.3817	27.3586	24.5237	23.61785
CG43082	19.0736	28.5308	36.9	9.87545	13.2884	15.801	20.57821
CG43448	5.40864	6.09305	8.10556	6.00727	9.40819	5.87862	6.816888
CG43725	22.1981	25.4976	21.9507	18.4631	15.6888	16.7318	20.08835
CG44006	8.44461	41.5696	45.037	64.3692	37.3677	74.2565	45.1741
CG4496	26.2706	24.1444	29.3513	8.89722	11.0688	6.14749	17.64664
CG4580	6.00383	5.20566	5.23901	2.72661	7.4807	8.5033	5.859852
CG4797	8.32395	7.42282	7.70943	3.80848	3.83741	3.77273	5.81247
CG4950	45.942	54.5634	53.8963	50.7859	61.4007	54.3869	53.49587

CG6421	4.48388	3.60569	4.67008	12.3101	14.9158	8.47293	8.076413
CG6553	330.812	240.955	287.818	157.1	15.6539	27.8154	176.6924
CG8012	68.7798	64.6098	61.5197	67.4075	104.677	66.2938	72.2146
Cht8	33.8203	22.9078	27.1052	30.6399	27.7485	26.0511	28.04547
Cpr47Ee	3.20869	2.89745	2.90747	4.5258	4.82173	3.3653	3.621073
Cpr72Ea	4631.67	2807.27	3803.3	3695.75	2982.04	3092.04	3502.012
Cpr72Eb	4631.67	0	7.37099	0	3.65331	6.02967	774.7873
CR41544	38.4122	18.7714	26.92	80.0688	29.3095	84.0779	46.25997
CR43701	8.00734	0	115.191	0	0	68.6634	31.97696
CR44604,CR44605	21.722	14.4087	18.8143	11.9541	21.3252	15.3177	17.257
CR45232	4.53977	23.9349	8.50866	34.1961	6.57248	13.1644	15.15272
CR45600	33.0499	43.2947	36.8608	36.4881	48.6266	61.4911	43.30187
CR45737	5.07844	4.93209	7.14644	3.56011	3.10189	3.48687	4.550973
DptA	3.24118	4.24782	13.2913	0.924797	6.89364	3.16556	5.29405
Dro	14.9926	10.0924	23.2394	63.7668	93.7417	94.2071	50.00667
Drsl5	138.784	125.756	219.896	128.513	93.9049	39.6514	124.4176
Eig71Ej	27.6986	44.0089	65.0456	20.635	21.2789	39.3942	36.34353
Eip93F	2.80604	17.9562	6.70127	7.69271	6.46317	35.3255	12.82415
fau	6.15186	7.00017	5.80747	10.3039	8.41686	9.99154	7.9453
Fbp2	75.0319	71.7803	193.07	35.3594	92.0936	97.5579	94.14885
fru	3.3115	9.80378	6.71948	8.68304	4.59166	6.72271	6.638695
IM3	12.0208	23.7347	23.2832	27.2316	58.9363	22.2028	27.90157
Jhe	3.59572	2.65032	4.32216	2.69033	3.69051	4.10946	3.50975
lectin-24Db	32.2829	24.0328	31.8746	22.5425	0	0	18.45547
Lsp1alpha	6.68228	5.79305	20.3675	2.0164	4.7389	4.21213	7.30171
Lsp1beta	22.461	15.32	47.9024	13.9318	19.2016	18.9075	22.95405
mamo	1.48762	15.2982	2.83053	5.25341	41.8556	10.7414	12.91113
Mur89F	63.5851	120.22	64.3406	149.213	73.6929	178.918	108.3283
NimC2	53.7058	49.2815	39.8242	54.0128	67.7624	53.4852	53.01198
NimC3	260.394	194.27	222.263	112.968	161.835	121.885	178.9358
Osi11	4.97632	4.05171	19.0135	6.27703	4.89506	3.72879	7.157068
Osi22	4.39555	4.79839	8.76835	4.41896	6.56605	3.65971	5.434502
Osi8	7.10182	3.25949	11.9223	3.91733	2.49224	1.46114	5.02572
ppk13	7.94274	16.0548	10.6211	5.50644	4.08754	6.30201	8.419105
rdhB	3.64268	2.7908	3.94228	4.36937	4.80464	3.93481	3.914097
snoRNA:Psi28S-3342	6.5511	3.66948	109.21	28.6329	6.28464	18.7692	28.85289
snRNA:U5:14B	9.0314	5.06337	8.2457	5.87782	50.9656	8.78964	14.66226
snRNA:U5:63BC	140.03	0	294.851	0	148.669	156.533	123.3472
Spn47C	9.55095	9.34919	10.9781	11.4258	12.6297	15.9666	11.65006
stum	2.93424	2.65061	3.34775	3.65469	3.4325	3.41567	3.239243
TotA	12.8166	13.1726	27.0179	10.0839	14.3767	16.6129	15.6801
TotB	9.99221	7.77381	16.5611	8.0071	11.1032	10.1884	10.6043
tRNA:SeC-TCA-1-1	0	2.5383	414.822	0	2.72805	0	70.01473
Ugt86Di	5.06777	3.60708	4.97671	2.69517	3.39641	2.66275	3.734315
upd2	1.85191	2.45025	2.68252	2.49175	3.69666	3.07775	2.708473

Supplementary File 1. FPKM values (with high and low confidence values) after transcriptome assembly with cufflinks for Oregon R replicate 1.

Supplementary File 2. FPKM values (with high and low confidence values) after transcriptome assembly with cufflinks for Oregon R replicate 2.

Supplementary File 3. FPKM values (with high and low confidence values) after transcriptome assembly with cufflinks for Oregon R replicate 3.

Supplementary File 4. FPKM values (with high and low confidence values) after transcriptome assembly with cufflinks for *e,wo,ro* replicate 1.

Supplementary File 5. FPKM values (with high and low confidence values) after transcriptome assembly with cufflinks for *e,wo,ro* replicate 2.

Supplementary File 6. FPKM values (with high and low confidence values) after transcriptome assembly with cufflinks for *e,wo,ro* replicate 3.

Supplementary File 7. FPKM values (with high and low confidence values) for both Oregon R and *e,wo,ro* after comparison with cuffdiff.

Supplementary File 8. Oregon R *svb* locus ATAC-seq peaks (called with MACS2) with information about position, summit position, height, -log10 (p and q values), and enrichment.

Supplementary File 9. *e,wo,ro svb* locus ATAC-seq peaks (called with MACS2) with information about position, summit position, height, -log10 (p and q values), and enrichment.